



**HAL**  
open science

## A comparison of smooth basis constructions for isogeometric analysis

H.M. Verhelst, Pascal Weinmüller, Angelos Mantzaflaris, Thomas Takacs,  
Deepesh Toshniwal

► **To cite this version:**

H.M. Verhelst, Pascal Weinmüller, Angelos Mantzaflaris, Thomas Takacs, Deepesh Toshniwal. A comparison of smooth basis constructions for isogeometric analysis. *Computer Methods in Applied Mechanics and Engineering*, 2023, 419, pp.116659. 10.1016/j.cma.2023.116659 . hal-04313467v2

**HAL Id: hal-04313467**

**<https://hal.science/hal-04313467v2>**

Submitted on 15 Oct 2024

**HAL** is a multi-disciplinary open access archive for the deposit and dissemination of scientific research documents, whether they are published or not. The documents may come from teaching and research institutions in France or abroad, or from public or private research centers.

L'archive ouverte pluridisciplinaire **HAL**, est destinée au dépôt et à la diffusion de documents scientifiques de niveau recherche, publiés ou non, émanant des établissements d'enseignement et de recherche français ou étrangers, des laboratoires publics ou privés.

# A comparison of smooth basis constructions for isogeometric analysis

H.M. Verhelst<sup>a,b,\*</sup>, P. Weinmüller<sup>c</sup>, A. Mantzaflaris<sup>d</sup>, T. Takacs<sup>e</sup>, D. Toshniwal<sup>a</sup>

<sup>a</sup>*Delft University of Technology, Department of Applied Mathematics, Mekelweg 4, Delft 2628 CD, The Netherlands*

<sup>b</sup>*Delft University of Technology, Department of Maritime and Transport Technology, Mekelweg 2, Delft 2628 CD, The Netherlands*

<sup>c</sup>*MTU Aero Engines AG, Dachauer Straße 665, 80995, Munich, Germany*

<sup>d</sup>*Inria centre at Université Côte d'Azur, 2004 route des Lucioles - BP 93, 06902 Sophia Antipolis, France*

<sup>e</sup>*Johann Radon Institute for Computational and Applied Mathematics, Austrian Academy of Sciences, Altenberger Str. 69, 4040 Linz, Austria*

---

## Abstract

In order to perform isogeometric analysis with increased smoothness on complex domains, trimming, variational coupling or unstructured spline methods can be used. The latter two classes of methods require a multi-patch segmentation of the domain, and provide continuous bases along patch interfaces. In the context of shell modeling, variational methods are widely used, whereas the application of unstructured spline methods on shell problems is rather scarce. In this paper, we therefore provide a qualitative and a quantitative comparison of a selection of unstructured spline constructions, in particular the D-Patch, Almost- $C^1$ , Analysis-Suitable  $G^1$  and the Approximate  $C^1$  constructions. Using this comparison, we aim to provide insight into the selection of methods for practical problems, as well as directions for future research. In the qualitative comparison, the properties of each method are evaluated and compared. In the quantitative comparison, a selection of numerical examples is used to highlight different advantages and disadvantages of each method. In the latter, comparison with weak coupling methods such as Nitsche's method or penalty methods is made as well. In brief, it is concluded that the Approximate  $C^1$  and Analysis-Suitable  $G^1$  converge optimally in the analysis of a bi-harmonic problem, without the need of special refinement procedures. Furthermore, these methods provide accurate stress fields. On the other hand, the Almost- $C^1$  and D-Patch provide relatively easy construction on complex geometries. The Almost- $C^1$  method does not have limitations on the valence of boundary vertices, unlike the D-Patch, but is only applicable to biquadratic local bases. Following from these conclusions, future research directions are proposed, for example towards making the Approximate  $C^1$  and Analysis-Suitable  $G^1$  applicable to more complex geometries.

*Keywords:* Isogeometric Analysis, Unstructured Splines, Kirchhoff–Love shell, Biharmonic Equation

---

\*Corresponding Author.

*Email addresses:* h.m.verhelst@tudelft.nl (H.M. Verhelst), pascal.weinmueller@mtu.de (P. Weinmüller), angelos.mantzaflaris@inria.fr (A. Mantzaflaris), thomas.takacs@ricam.oeaw.ac.at (T. Takacs), d.toshniwal@tudelft.nl (D. Toshniwal)

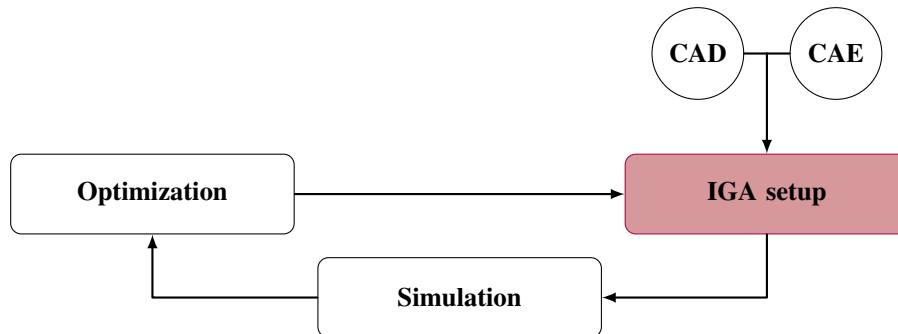


Figure 1: General workflow for solving a physics problem and optimizing a geometry or topology coming from CAD and CAE processes. Starting from *CAD* and *CAE*, the *IGA Setup* is performed. In this block, a computational basis is extracted from the geometry, to be used for simulation. Then, the *Simulation* block involves assembly of the operators of the physics problem on the computational basis coming from the *IGA Setup*. In case of shape or topology optimization problems, the simulation results are evaluated and the shape/topology is modified. From this changed shape/topology, a new computational basis can be obtained and the process can be repeated. The *IGA Setup* block is marked to be elaborated further on in Fig. 2.

## 1. Introduction

Present day engineering disciplines depend on Computer-aided design (CAD) and numerical simulation models for physics for design and analysis. Typically, geometries designed in CAD are converted to meshes for an analysis with numerical techniques like Finite Element Methods (FEMs). Since the geometry description in CAD is based on splines whereas meshes for simulation are based on linear geometry approximations, geometric data is lost during this conversion. Isogeometric analysis [1] is the bridge between CAD and Computer-Aided Engineering (CAE), since it is employing splines as a basis for geometric design and numerical analysis. In practice, an isogeometric analysis and optimization workflow can be seen as depicted in Fig. 1. Starting with a geometry from CAD as well as from material parameters, boundary conditions et cetera from CAE, isogeometric simulations and eventually geometry or topology optimization can be performed. The step connecting the inputs from CAD and CAE is referred to as *IGA Setup* in Fig. 1. This step takes care of the preparation for the simulation step, including the pre-processing of the geometry, if needed, and the construction of the isogeometric discretization space.

Due to the arbitrary smoothness of spline basis functions, isogeometric analysis has several advantages over conventional finite element methods. For example: (i) the introduction of  $k$ -refinements, which are proven to provide high accuracy per degree of freedom [2, 3]; (ii) high accuracy in eigenvalue problems, e.g. for structural vibrations [4–6]; or (iii) geometric exactness in parametric design and interface problems, e.g. applied to the parametric design of prosthetic heart valves [7]. Furthermore, the  $C^1$ -smooth discretization spaces allow to solve equations such as the biharmonic equation, the Cahn–Hilliard equations or the Kirchhoff–Love shell equations without introducing auxiliary variables. However, due to the tensor-product structure of the spline basis, higher-order smoothness can be enforced easily only on domains that allow simple patch partitions (e.g. an L-shape or an annulus), whereas on geometrically and topologically more complicated domains alternative approaches are required to solve equations that require basis functions of higher-order continuity.

29 For more complicated domains, the *IGA setup* block in Fig. 1 involves a pre-processing step  
30 of either the geometry, the system of equations or the solution space to solve the original sys-  
31 tem of equations. In Fig. 2, this pre-processing step is subdivided into three options: trimmed  
32 domain approaches, unstructured splines and variational coupling methods. Given an initial ge-  
33 ometry (cf. Fig. 3a), the trimmed domain approaches alter the tensor-product domain by defining  
34 parts of the domain that are physical or non-physical (cf. Fig. 3b). In case of unstructured splines  
35 or variational coupling methods, the geometry is decomposed into multiple different patches (cf.  
36 Fig. 3c) on which continuity conditions are enforced by constructing a smooth basis (unstructured  
37 splines) or by adding extra terms to the system of equations (variational coupling approaches). In  
38 Section 2 of this paper, a review of trimmed domain approaches, unstructured splines and varia-  
39 tional coupling methods is provided. Examples include immersed methods, degenerate patches  
40 and Nitsche’s method, respectively. In case of simple geometries (and given the right inputs) the  
41 methods are identical.

42  
43 As shown in Fig. 2, each class of methods has its own characteristics and previous work  
44 has provided several comparisons of methods among each other, which are elaborated more in  
45 Section 2. In the context of the workflow sketched in Fig. 1, unstructured splines provide a  
46 valuable alternative to the other methods, since they are constructed for a fixed topology and  
47 hence the computational costs of their construction are not related to changing shapes or moving  
48 domains. However, recent developments mainly focused on different unstructured spline meth-  
49 ods separately, rather than providing a valuable comparison. In this paper, we therefore provide  
50 a qualitative and a quantitative comparison of a selection of unstructured spline constructions.  
51 We consider finite, piece-wise polynomial spline constructions, hence we do not include ratio-  
52 nal constructions or infinite representations, such as subdivision surfaces. More precisely, we  
53 compare examples of (globally)  $G^1$ -smooth multi-patch constructions (the Analysis-Suitable  $G^1$   
54 construction of [8] and the Approximate  $C^1$  construction of [9]), the D-Patch method of [10] and  
55 the Almost- $C^1$  construction of [11], motivated in Section 2.3. The selected methods are qualita-  
56 tively compared based on their properties, and quantitatively based on several different examples  
57 with biharmonic and Kirchhoff–Love shell equations. The aim of this paper is to provide a fair  
58 comparison<sup>1</sup> of these methods, providing a good overview of the strengths and weaknesses of  
59 each method in different cases.

60  
61 The paper is outlined as follows: in Section 2, a detailed overview of the methods appearing  
62 in Fig. 2 is provided. In Section 3 we provide a qualitative analysis of the four constructions that  
63 are discussed in this paper, while in Section 4 we provide a quantitative analysis of all methods.  
64 There, we present five benchmark problems solving either a biharmonic or a Kirchhoff–Love  
65 equation. These benchmark problems serve different purposes and we compare which method,  
66 in which setting, performs best. In Section 5, we conclude this paper based on the findings from  
67 the previous sections and we provide directions for future research.

68

---

<sup>1</sup>We believe that a comparison like the one presented in this paper is never fully unbiased, since the authors have contributed to different methods in previous publications and do not represent the entire research community.



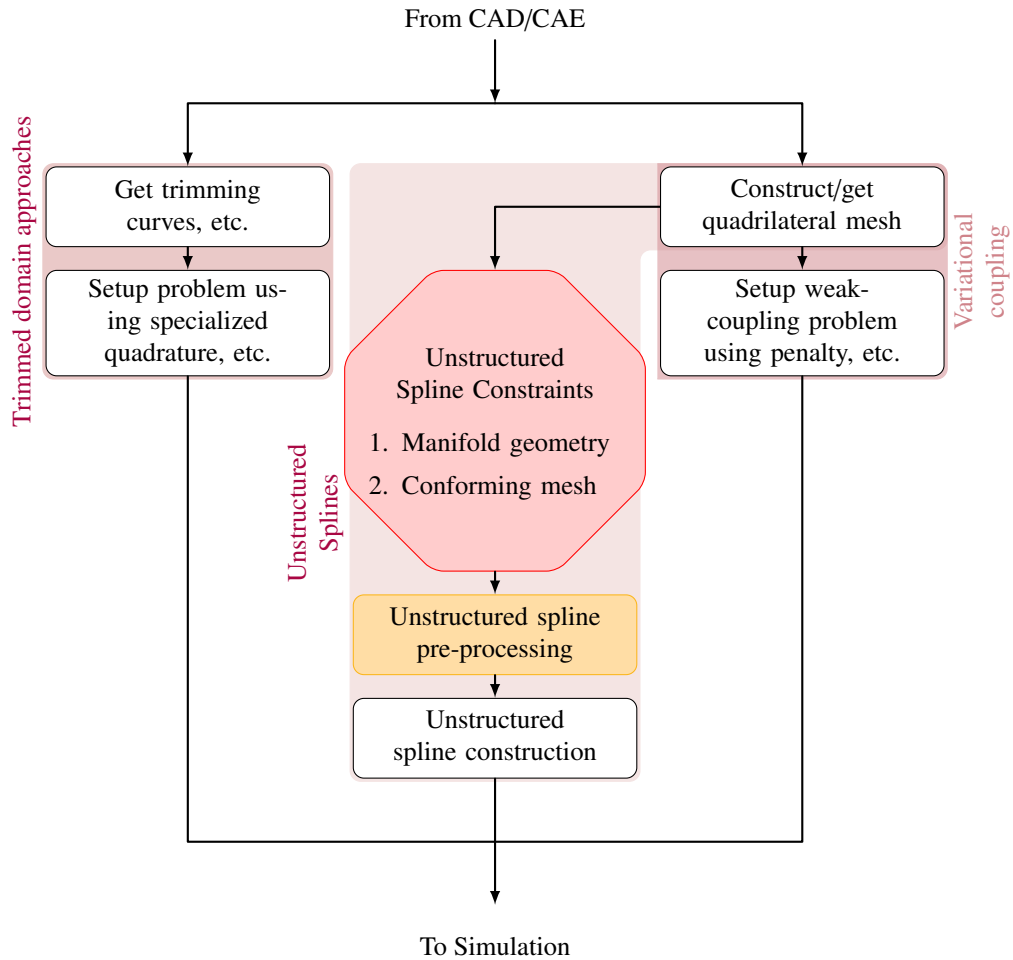


Figure 2: Inside the *IGA Setup* block from Fig. 1, three methods are distinguished. Firstly, *trimmed domain approaches* use trimming curves or surfaces to identify parts of a tensor-product domain as the actual domain. However, since elements can be trimmed poorly, *specialized quadrature* rules and solver preconditioners are typically needed. Alternatives to trimming are *weak coupling* or *unstructured spline* methods. For both classes of methods, a geometry with a given topology needs to be decomposed into multiple sub-domains (i.e. patches) via *quadrilateral meshing*. Given a quadrilateral mesh, *weak methods* assemble extra penalty terms into the equation to be solved, or add extra equations to be solved to satisfy continuity constraints. Lastly, *unstructured spline* constructions can be used to couple multiple domains by constructing a continuous basis. These methods, however can only be used on *manifold geometries* and *conforming meshes*. When these requirements are satisfied, *unstructured spline pre-processing* is required before the *unstructured spline construction* can take place. The *pre-processing* is highlighted and will be elaborated on more in Fig. 7 in Section 3.

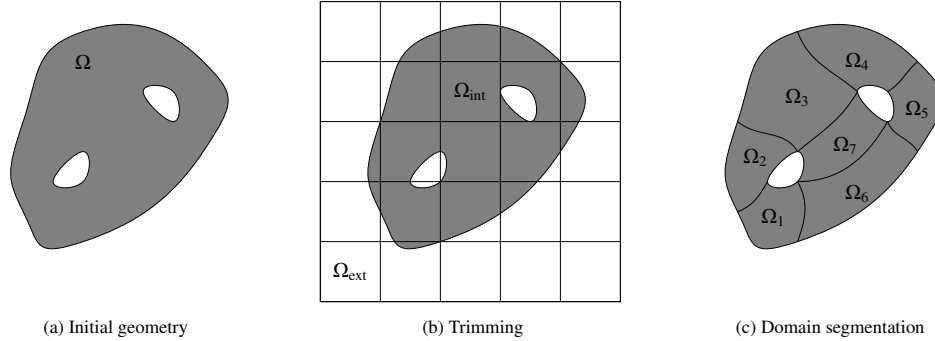


Figure 3: Given an initial geometry  $\Omega$  (a), trimming (b) uses the curves of the boundary of the original geometry to define the interior domain  $\Omega_{\text{int}}$  and the exterior domain  $\Omega_{\text{ext}}$ . An alternative approach for modelling the domain is to use domain segmentation (c). Here, the domain is decomposed into several patches  $\Omega_i$  which together define the full domain  $\Omega$ .

## 69 2. Multi-patch isogeometric analysis: literature review

70 As discussed in the introduction of this paper, in particular in Fig. 2, three classes of methods  
 71 for the modelling of complicated domains can be characterised: trimmed domain approaches,  
 72 variational coupling methods and unstructured splines. The goal of all methods is to achieve a  
 73 certain level of continuity across the whole analysis domain such that multi-patch isogeometric  
 74 analysis can be performed for example for the Kirchhoff–Love shell model [12], the biharmonic  
 75 equation or the Cahn–Hilliard equation [13]. As shown in Fig. 3, trimmed domain approaches  
 76 use the fact that parts of tensor-product geometries are trimmed away, using trimming curves to  
 77 separate regions of interest and regions that should be omitted, see Fig. 3b. Variational coupling  
 78 approaches and unstructured splines are defined on multi-patch domains, typically following  
 79 from a segmentation of the original domain, see Fig. 3c. In case of variational coupling methods,  
 80 the system of equations is enriched with terms that will enforce continuity (typically in a weak  
 81 sense) between the patches. In case of unstructured spline constructions, a basis is constructed  
 82 on the multi-patch object, where certain smoothness is enforced strongly. When starting from a  
 83 trimmed geometry, the step of creating a multi-patch domain decomposition (i.e. *untrimming*)  
 84 from an arbitrary geometry with an arbitrary topology is a very important step in the application  
 85 of weak coupling methods and unstructured spline constructions, as can be seen in the flowchart  
 86 in Fig. 2. In this paper, however, the topic of untrimming will not be discussed as it is out of  
 87 scope of our study. Hence, the reader is referred to [14, 15] for an overview of these methods.

88  
 89 In this section, an overview of the trimmed domain approaches (Section 2.1), variational cou-  
 90 pling methods (Section 2.2) and unstructured splines (Section 2.3) is provided. A fourth method,  
 91 which will not be discussed in this section, is to introduce auxiliary variables for derivatives of  
 92 the solution, so that  $C^1$  continuity requirements are reduced to  $C^0$  and standard interface coupling  
 93 can be used. These so-called mixed formulations are common in conventional FEM, although  
 94 recent advances have also been made for Kirchhoff–Love plates and shells and the biharmonic  
 95 eigenvalue problem [16–18].

### 96 2.1. Trimming approaches

97 Trimming is a technique where so-called trimming curves or surfaces separate parts of tensor-  
 98 product spline domains to define a geometry. Trimming is a common technique to represent

99 complex geometries in CAD, and typically geometries consist of multiple trimmed patches with  
100 boundary and interface curves trimming the actual patches. We refer to the work [19] for an  
101 overview of trimming methods in isogeometric analysis. Generalizing the idea of trimming to  
102 techniques where curves or surfaces are used to define the domain of interest as *trimmed domain*  
103 *approaches*, several approaches have been proposed to perform simulations on complex geome-  
104 tries, including the finite cell method [20–22], Cut-FEM [23] or immersed methods [24, 25].  
105 The advantage of these methods is that the trimmed CAD geometries could directly be used for  
106 analysis. However, when only small parts of the physical domain are cut, leading to small cut  
107 elements, numerical difficulties can occur in the conditioning of the system, leading to solver  
108 instabilities or accuracy problems [26]. Therefore, the analysis of complex trimmed geome-  
109 tries via methods like the FCM typically require special quadrature schemes to take into account  
110 small cut cells [27] or preconditioners to stabilize the numerical analysis [28]. In the context  
111 of Kirchhoff–Love shell modelling, isogeometric analysis on trimmed geometries has been per-  
112 formed in several studies [29–31] including some with focus on multi-patch coupling [31–35].

113

## 114 2.2. Variational coupling methods

115 We define variational coupling methods as methods that modify the system of equations to  
116 enforce certain continuity across patch interfaces. Examples of these methods are penalty meth-  
117 ods, Nitsche’s methods, mortar methods or Lagrangian penalized methods. In the context of  
118 Kirchhoff–Love shell analysis, these weak coupling methods have received a lot of attention in  
119 previous studies and an overview is provided by [36]. Firstly, an in-plane coupling was proposed  
120 in [37] together with a method for coupling non-manifold patches using the so-called bending  
121 strip method [38]. Later, weak coupling approaches have been developed for multi-patch do-  
122 mains. Here, coupling terms can be added inside the existing variational formulation (referred  
123 to as Nitsche’s or penalty methods) or imposed by Lagrange multipliers (referred to as mortar  
124 methods).

125

126 Several works on Nitsche techniques (cf. [39]) for isogeometric analysis have been published  
127 starting from the imposition of boundary conditions [40], towards multi-patch coupling and the  
128 coupling of patches [41], later using a non-symmetric parameter-free Nitsche’s method [42].  
129 Nitsche’s methods have been applied to Kirchhoff plates [43], Kirchhoff–Love shells [29, 44, 45],  
130 hyperelastic 2D elasticity [46] and the biharmonic equation [9, 47] and for modelling local sub-  
131 domains [48] for elasticity simulations. The advantages of Nitsche’s methods are that the for-  
132 mulation is variationally consistent and requires only mild stabilization, which can be performed  
133 automatically, by estimating the stability parameter. However, the involved integral terms are  
134 complicated expressions that impose high implementation and assembly efforts. Therefore, cou-  
135 pling approaches using only penalization have been developed [49–53]. Although several im-  
136 provements have been made in these works, the main disadvantage of penalty methods is that  
137 a suitable penalty parameter has to be chosen. Using the super penalty approach [33, 54], the  
138 computation of the penalty parameter can be automated. However, this method has not yet been  
139 tested for non-linear shell problems or on ‘dirty’ geometries. Both Nitsche’s and penalty methods  
140 can be used to couple geometries that are non-manifold, i.e. geometries that have out-of-plane  
141 connections like stiffened structures by penalizing changes in the angle of patches on an inter-  
142 face. Furthermore, the methods can handle interfaces with non-matching parameterizations.

143

144 Instead of adding coupling terms in the variational form, as is done in Nitsche’s and penalty  
145 methods, mortar methods [55] add extra degrees of freedom by introducing Lagrange multipli-  
146 ers which are required to resolve additional coupling conditions. The use of mortar methods to  
147 couple non-conforming isogeometric sub-domains was first done by [56]. In [57] the FEA-based  
148 approach of [55] was extended for NURBS-based IGA, but the aim was to develop a method  
149 for  $C^0$ -coupling for Reissner-Mindlin shells, hence insufficient for isogeometric Kirchhoff–Love  
150 shells. A mortar method aiming to establish  $C^1$  coupling is given in [58] and a method that  
151 provides  $C^n$  continuity was given by [59, 60]. Furthermore,  $G^1$  mortar coupling, referred to as  
152 extended mortar coupling, was presented in [61] for Kirchhoff–Love shells, based on a coupling  
153 in least square sense. On the other hand, in [62] a mortar method to enforce  $C^1$  coupling for  
154 the biharmonic equation was developed, where the Lagrange multiplier spaces are constructed  
155 similarly to [63] for  $C^0$ -coupling. An approach to reduce computational costs involved in finding  
156 Lagrange multipliers is called dual mortaring [64], where Lagrange multipliers are eliminated  
157 using a compact dual basis. This approach has been developed for Bezier elements [65] and it  
158 has been applied for Kirchhoff–Love shells [66] and a bi-orthogonal spline space has been pre-  
159 sented for weak dual mortaring for patch coupling [67]. In [68], a hybrid method was provided  
160 and applied to Kirchhoff plates, which combines mortar methods and penalty methods. Lastly,  
161 a comparison of Nitsche, penalty and mortar methods is given by [69]. For a more complete  
162 overview of mortar methods for isogeometric analysis, the reader is referred to [70]. In gen-  
163 eral, mortar methods have the advantage over Nitsche’s methods that there are no parameters  
164 involved and that the implementation efforts are lower. However, the disadvantage is that a suit-  
165 able spline space needs to be found for the Lagrange multipliers [62, 63, 71]. Like Nitsche’s and  
166 penalty methods, mortar methods can handle non-matching parameterizations and non-manifold  
167 interfaces, the latter by similar penalization of interfacing patches.

### 168 2.3. Unstructured splines

169 Compared to weak coupling methods, unstructured spline constructions do not alter the sys-  
170 tem of equations to be solved. Instead, the computational basis is modified such that it satisfies  
171 continuity conditions across patch interfaces. Unstructured splines are typically constructed for  
172 in-plane (i.e. manifold) interfaces and not on out-of-plane (i.e. non-manifold) interfaces, since  
173 the notion of smoothness is uniquely defined only in the former setting. However, unstructured  
174 spline constructions for non-manifold interfaces are possible, e.g. as in [72–74] in the con-  
175 text of subdivision. Furthermore, unstructured spline constructions are typically constructed on  
176 conforming interfaces, i.e. interfaces with matching meshes, but, as long as the patch param-  
177 eterizations are matching, this can be overcome by taking the knot vector union of the interface  
178 patches. However, the advantage of unstructured spline constructions is that as soon as the basis  
179 is constructed for a certain untrimmed geometry, there are no additional costs involved other than  
180 evaluation costs for changing shapes, which make unstructured spline bases suitable for shape  
181 optimization problems. In case of topology changes or large changes of the shape, however, the  
182 mesh topology of the unstructured spline space has to be changed as well. Unlike weak methods,  
183 which are typically based on the introduction of penalties (e.g. in terms of energy), unstructured  
184 spline constructions are typically provided as generic geometric methods that are applicable to  
185 any equation that requires  $C^1$  coupling across multi-patch interfaces. With the advance of isoge-  
186 ometric analysis, the interest in parametrically  $C^1$  and geometrically  $G^1$  splines has grown. An  
187 overview of smooth multi-patch discretizations for isogeometric analysis can be found in [75],  
188 and a small overview is provided below. We distinguish between enforcing parametric conti-  
189 nuity, i.e., the type of continuity between mesh elements within a regular tensor-product spline

190 patch, and general geometric continuity, cf. [76]. In the following, three types of constructions  
191 are classified, depending on their continuity on patch interfaces, around vertices and in the patch  
192 interior:

- 193 • Patch coupling with geometric continuity on patch interfaces and parametric continuity  
194 inside patches.
- 195 • Patch coupling with parametric continuity everywhere.
- 196 • Patch coupling with parametric continuity almost everywhere.

197 Although other constructions outside of these categories exist, e.g., [77, 78], our review is  
198 restricted to the aforementioned categories since the methods considered in Sections 3 and 4 fall  
199 into these categories.

#### 200 *Geometric continuity on patch interfaces and parametric continuity inside patches*

201 This first category of unstructured spline constructions assumes that a fixed  $C^0$ -matching  
202 multi-patch parametrization is given. On this multi-patch domain, a  $C^1$ -smooth isogeometric  
203 space is constructed. As shown in [76], for any isogeometric function the  $C^1$  condition over each  
204 interface is equivalent to a  $G^1$  geometric continuity condition of the graph surface correspond-  
205 ing to the function. If the domain is planar and the patches are bilinear, then the  $C^1$  constraints  
206 can be resolved and a  $C^1$  spline space was constructed by [79] and applied to the isogeometric  
207 analysis of the biharmonic equation in [80]. It could be shown in [81] and [82] that  $C^1$  splines  
208 over bilinear quadrilaterals and mixed (bi)linear quadrilateral/triangle meshes possess optimal  
209 approximation properties. Furthermore, the work [83] studied the arbitrary  $C^n$ -smooth spline  
210 space for bi-linear multi-patch parameterizations, based on their previously published findings.

211  
212 Considering general  $C^0$ -matching multi-patch domains, the work of [84] introduces the class  
213 of analysis-suitable  $G^1$  (AS- $G^1$ ) multi-patch parameterizations which includes bi-linear patches.  
214 This AS- $G^1$  condition is in general required to obtain optimal approximation properties. The  
215 condition implies that the gluing data for  $G^1$  continuity is linear, which is explained in more  
216 detail in Section 3.1. While it could be shown in [85] that all planar multi-patch domains possess  
217 AS- $G^1$  reparameterizations, creating AS- $G^1$  surface domains is more difficult. Several strategies  
218 to achieve this were introduced in [8], thus making  $C^1$ -smooth multi-patch parameterizations  
219 applicable to biharmonic equations and isogeometric Kirchhoff–Love shell models [86]. In the  
220 work of [87] the construction of [84] is used to develop a scaled-boundary model for smooth  
221 Kirchhoff–Love shells, similar to the approach of [88] for Kirchhoff plates.

222  
223 Alternatively to constructing an AS- $G^1$  parameterization, one can relax the smoothness con-  
224 ditions. This was done in [9], where the construction of an approximate  $C^1$  (Approx.  $C^1$ ) space  
225 is presented. The basis construction is explicit, possesses the same degree-of-freedom structure  
226 as an AS- $G^1$  space, but the  $C^1$  condition is not satisfied exactly but only approximately. It de-  
227 faults to the AS- $G^1$  construction when the AS- $G^1$  requirements are met. In [47] a comparison of  
228 the presented space with Nitsche’s method was performed, yielding optimal convergence results  
229 without the need of a coupling terms. More details on the Approx.  $C^1$  method are provided in  
230 Section 3.2.

231

232 *Parametric continuity everywhere*

233 The starting point for this class of constructions is different from the previous. Here we cre-  
234 ate smooth splines in a parametric sense between neighboring mesh elements. Such parametric  
235  $C^1$  conditions are easy to resolve, but they lead to singularities at vertices of valencies other than  
236 four, so-called extraordinary vertices. This is due to the conflicting coupling conditions on partial  
237 derivatives around the EVs, which lead to all partial derivatives to vanish there. Inspired by the  
238 Degenerate Patch (D-Patch) approach from [89], the works of [10, 90] provide  $C^1$  smooth spline  
239 spaces for multi-patch geometries with parametric smoothness everywhere. On extraordinary  
240 vertices (EVs), which is a junction between 3 or 5 or more patches (i.e. valence  $\nu > 2, \nu \neq 4$ ), the  
241 original D-Patch method shows a singularity of the basis in EVs combined with a reduction of  
242 degrees of freedom in this point. An improvement of the D-Patch method was presented in [90],  
243 by splitting elements around the EVs such that every element is associated to four degrees of  
244 freedom. However, this construction does not have non-negativity and is based on PHT splines,  
245 which have limited smoothness. A new design and analysis framework for multi-patch geome-  
246 tries was presented in [10], based on D-Patches with T-splines for refinement and non-negative  
247 splines yielding optimal convergence properties. This was also demonstrated in [91] for isoge-  
248 ometric Kirchhoff–Love shells. In the work [92], it is motivated that this construction can also  
249 be used if only one element around the EV is isolated. More details on the D-Patch method are  
250 provided in Section 3.3.

251  
252 Alternatively, subdivision surface based constructions lead to unstructured splines that are  
253 parametrically continuous everywhere, cf. [93–97]. However, such approaches require an infi-  
254 nite number of polynomial pieces around each EV. Thus, we discard them for our comparison.  
255 Moreover, in general their approximation properties are severely reduced near EVs [98].

257 *Parametric continuity almost everywhere*

258 As mentioned previously, imposing parametric continuity everywhere leads to singularities  
259 at all EVs. Thus, instead of constructing a space with full parametric continuity, spaces with  
260 parametric continuity almost everywhere except around the EVs can also be considered. This  
261 way, one ends up with regular, smooth rings around EVs which then need to be filled in some  
262 way. Such so-called *hole-filling* techniques are commonplace in geometric modeling and can  
263 also be used to construct smooth spaces for isogeometric analysis, cf. [99–104]. We focus here  
264 on the simplest possible way of resolving this issue, which is to enforce only  $C^0$ -smoothness  
265 near the EVs and  $G^1$  at the EV, namely the Almost- $C^1$  construction proposed in [11]. Simi-  
266 lar constructions, which enforce no additional smoothness near EVs were proposed for mixed  
267 quadrilateral/triangle meshes in [105] and for arbitrary degree multi-patch B-splines with en-  
268 hanced smoothness (MPBES) in [106].

269  
270 The Almost- $C^1$  construction we consider here yields piece-wise biquadratic splines which  
271 are  $C^1$  in regular regions and which have reduced smoothness around extraordinary vertices, in-  
272 dependent of the valence or the location (i.e. interior or boundary EVs). In contrast to that, most  
273 commonly used hole-filling approaches yield exactly  $C^1$ -smooth spaces but introduce locally  
274 polynomials of higher degree, or require a higher degree to start with, such as the construction  
275 presented in [107], which converts Catmull–Clark subdivision surfaces to  $G^1$ -smooth piece-wise  
276 biquintic elements. While exact smoothness is of relevance for geometric modeling, it is not

277 necessary from an analysis point of view.

278

### 279 3. Qualitative comparison

280 In the qualitative comparison of this paper, we focus on the properties of different unstruc-  
281 tured spline constructions and their implication on the application of these constructions in a  
282 workflow as in Fig. 1. More precisely, we comment on the continuity of each construction and  
283 their nestedness properties and we aim to provide a set of requirements for the *unstructured*  
284 *spline pre-processing* block in Fig. 2. Since the qualitative comparison of the considered meth-  
285 ods in this paper mostly covers properties of the methods and their implications, mathematical  
286 details about the construction or convergence properties are not provided. For more details, the  
287 reader is referred to [8] for the Analysis-Suitable  $G^1$  (AS- $G^1$ ) method, which extends the 2D  
288 construction from [108], to [9] for the Approximate  $C^1$  (Approx.  $C^1$ ) method, to [10] for the De-  
289 generate Patches (D-Patch) and to [11] for the Almost- $C^1$  method. However, for the qualitative  
290 comparison, some key terms are introduced as preliminaries.

291

292 Firstly, a *quadrilateral mesh* (*quad mesh*) is a mesh of quadrilateral elements, representing  
293 a (planar) surface geometry. The quadrilaterals can be represented by tensor B-splines of any  
294 degree which can be mapped onto a parametric unit-square. Typically, when the tensor B-spline  
295 quadrilaterals have different sizes in different directions or even different refinement levels, as-  
296 semblies of these *patches* are typically referred to as *multi-patches*. An example of a multi-patch  
297 is given in Fig. 3c. The conversion of a quad-mesh with many elements to a multi-patch with  
298 a smaller number of patches derived from groups of elements can be done using the procedure  
299 described in Fig. 4. Here, a half-edge mesh is traversed and elements are collected into groups  
300 corresponding to final patches. The vertices of the elements in one group (i.e. patch) form the  
301 control net of the bi-linear patch.

302

303 Secondly, for parametrically smooth constructions, different classes of vertices are consid-  
304 ered. For so-called *extraordinary vertices* (EVs), these constructions typically are different. An  
305 *interior extraordinary vertex* (*interior EV*) is a vertex on a quad mesh on which three or more  
306 than four patches meet. The number of patches coming together at a vertex is referred to as the  
307 *valence*, denoted by  $\nu$ . Furthermore a *boundary extraordinary vertex* (*boundary EV*) is a vertex  
308 on the boundary of the quad mesh with valence  $\nu \geq 3$ . For geometrically smooth constructions,  
309 the construction depends on the geometry around the vertex rather than the valence of the vertex.  
310 Hence, for these constructions the notion of EVs is irrelevant.

311

312 Lastly, a refinement of a spline space is called *nested* if the refined spline space is fully con-  
313 tained in the unrefined space. As a consequence, the geometry is exact under element refinement,  
314 which is beneficial from an analysis point of view.

#### 315 3.1. Analysis-suitable $G^1$

316 The analysis-suitable  $G^1$  (AS- $G^1$ ) construction is a novel approach in isogeometric analysis  
317 that was introduced for planar geometries and surfaces in [84], but a construction which extends  
318 [108] for planar domains to surfaces is detailed in [8]. This construction ensures that basis func-  
319 tions at interfaces have  $C^1$  continuity, while basis functions at vertices have  $C^2$  continuity. The



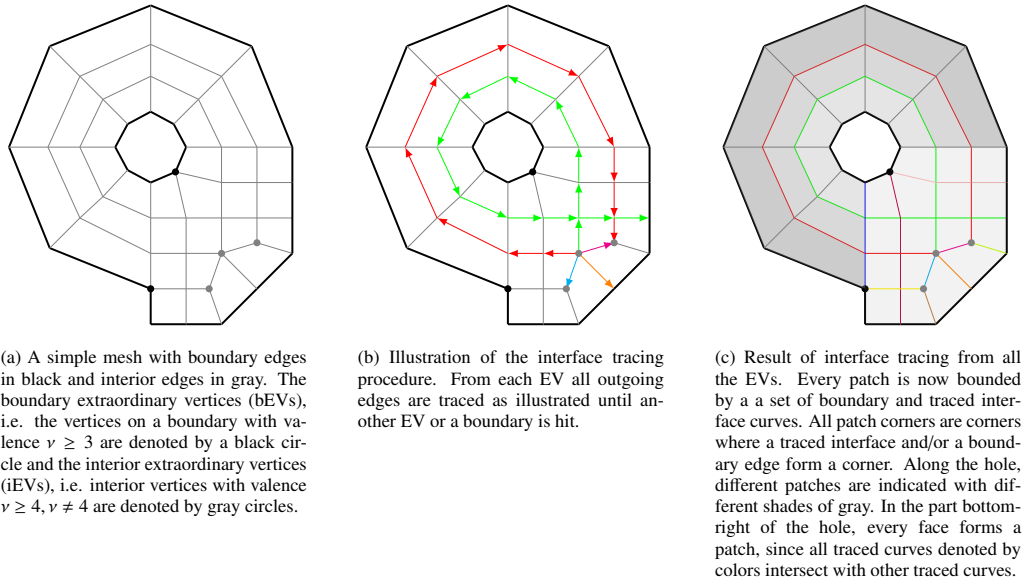


Figure 4: Procedure to find a multi-patch segmentation from a given mesh. The original mesh in (a) has 46 vertices, 81 edges and 45 faces and the final multi-patch (c) has 20 patches.

320 approach is based on the concept that  $G^k$ -smooth surfaces can produce  $C^k$ -smooth isogeometric  
 321 functions [76]. When dealing with general  $C^0$ -matching multi-patch domains, the so-called AS-  
 322  $G^1$  conditions must be satisfied to ensure optimal approximation. If these conditions are met,  
 323 a  $C^1$ -smooth subspace of the isogeometric space can be constructed, which is sufficiently large.  
 324 Such geometries are referred to as analysis-suitable geometries. However, it should be noted that  
 325 the  $C^1$ -smooth multi-patch isogeometric space generally depends on the geometry, as discussed  
 326 in [109]. To overcome this issue, an Argyris-like space was proposed in [108], which has a dimen-  
 327 sion that is independent of the geometry.

328  
 329 Given an interface between two patches, the  $C^1$  continuity condition at the interface is de-  
 330 fined by a linear combination of tangent vectors and transversal derivatives, which is referred to  
 331 as gluing data [84]. The  $C^1$  smooth basis functions at the interface, or more generally at the edge,  
 332 can be described by the first order Taylor expansion of the trace and the transversal derivative.  
 333 It is shown in [84], that the ideal choice for the space-representation of the trace and transver-  
 334 sal derivative is  $\mathcal{S}(\mathbf{p}, \mathbf{r} - 1, \mathbf{h})^2$  and  $\mathcal{S}(\mathbf{p} - 1, \mathbf{r} - 2, \mathbf{h})$ , respectively. These basis functions have  
 335 local support and are linearly independent, but they depend on the gluing data and, therefore,  
 336 on the geometry reparameterization itself. To ensure that the basis functions form a  $C^1$ -smooth  
 337 subspace of the isogeometric space, and to maintain the nestedness of the spline spaces, it is  
 338 necessary to have gluing data as a linear function which fulfils all analysis-suitable geometries.  
 339 For instance, all bi-linear patches meet this requirement. However, if a geometry is not analysis-  
 340 suitable, it can be reparameterized using the technique presented in [85].

<sup>2</sup>The notation  $\mathcal{S}(\mathbf{p} = (p, p), \mathbf{r} = (r, r), \mathbf{h} = (h, h))$  indicates a two-dimensional spline space with  $p$  as the polynomial degree,  $r$  as the regularity and  $h$  as the mesh size in both directions.



341

342 For any vertices in the quad mesh, to describe the  $C^1$  condition is not that straight-forward. In  
343 order to keep it general, the vertex basis functions is constructed by the  $C^2$  interpolation using the  
344  $C^1$  basis functions from the corresponding edges. As a consequence, the vertex basis functions  
345 also have local support and are linearly independent.

346

347 Summarizing, the AS- $G^1$  construction can be constructed by three different, linearly inde-  
348 pendent sub-spaces: interior, edge and vertex space. They can be described as follows:

349

- Interior space: basis functions that have zero values and derivatives on the patch edges and vertices.

350

351

- Interface space: basis functions that have vanishing function values up to the second derivatives at the vertices.

352

353

- Vertex space:  $C^2$  interpolating functions at the vertex, i.e., basis functions that have non-vanishing  $C^2$  data at the vertex.

354

355 The AS- $G^1$  construction with the interface and vertex constructions as described above are fully  
356  $C^1$  over the whole domain. In addition, the AS- $G^1$  construction can only be constructed when  
357 the degree of the basis is  $p \geq 3$  and the regularity is reduced as  $r \leq p - 2$ .

358

359 Figure 5a presents a local region around and EV with valence five with line styles indicating  
360 different continuity levels on patch or element boundaries (see the caption of Fig. 5). For the  
361 AS- $G^1$  construction, the continuity at the vertex is  $C^2$  by construction. Furthermore, the conti-  
362 nuity at the interior element interfaces is  $C^{p-2}$  due to the restriction on keeping the isoparametric  
363 concept. Lastly, since the AS- $G^1$  construction provides a  $G^1$  surface, the patch interfaces are  $C^1$   
364 by construction [76].

365

366

In sum, the core ideas behind the AS- $G^1$  construction are as follows:

367

- **Degree, regularity, continuity**

368

The spline space is fully  $C^1$ , hence suitable to solve fourth-order problems. However, the  
369 computation of the space requires analysis-suitability of the parameterization as well as  
370 degree  $p \geq 3$  and regularity  $r \leq p - 2$  for the basis functions.

371

- **Limitations on construction**

372

The space can be constructed on fully unstructured quadrilateral meshes with both interior  
373 and boundary extraordinary vertices. The construction of the basis functions is indepen-  
374 dent of the location or valence of the EVs. However, the analysis-suitability condition  
375 imposes a requirement on the geometries on which the construction can be constructed.  
376 Furthermore, the geometry parameterization is not changed.

377

- **Nestedness**

378

The spline spaces are nested.

379

- **Refinement procedure**

380

Refinement procedure is standard (by knot insertion) since the parameterization does not  
381 change.

382 *3.2. Approximate  $C^1$*

383 The Approximate  $C^1$  construction [9] provides, as the name suggests, approximately  $C^1$  con-  
 384 tinuity on interfaces and vertices, more precisely the construction provides  $C^1$  continuity in the  
 385 refinement limit. The Approx.  $C^1$  construction shares similarities with the AS- $G^1$  construction,  
 386 but the main difference between the construction of the Approx.  $C^1$  and the AS- $G^1$  spaces is that  
 387 it relaxes the AS- $G^1$  condition on the geometry, i.e., it allows geometries with non-linear gluing  
 388 data. In fact, the exact gluing data are splines with higher polynomial degree and lower regular-  
 389 ity or even piece-wise rational. As a consequence, trying to extend the construction for AS- $G^1$   
 390 parameterizations directly to non-AS- $G^1$  geometries yields complicated basis functions that are  
 391 challenging to evaluate and integrate accurately. To overcome this issue and obtain a construc-  
 392 tion with more easily definable basis functions, the gluing data are approximated. However, this  
 393 approximation means that the  $C^1$  condition is no longer satisfied exactly but only approximately.  
 394

395 By utilizing the approximation of the gluing data, the Approximate  $C^1$  construction incor-  
 396 porates the concept of different spline spaces found in the AS- $G^1$  construction. In this case, the  
 397 interior, vertex, and interface basis functions fulfill the same conditions as in the AS- $G^1$  con-  
 398 struction, but the degree and regularity differ between these spaces. Specifically, the sub-spaces  
 399 for the AS- $G^1$  construction have  $p \geq 3$  and  $r \leq p - 2$ , while the Approximate  $C^1$  construction  
 400 employs an interior space with  $p \geq 3$  and  $r \leq p - 1$ , along with vertex and interface spaces that  
 401 have locally reduced smoothness based on the approximation of the gluing data. Consequently,  
 402 on the one hand the Approximate  $C^1$  construction restores the potential for maximal smoothness  
 403 of isogeometric functions in the refinement limit, but the nestedness of the basis is lost. On the  
 404 other hand, the approximation of the gluing data in the Approximate  $C^1$  construction does not  
 405 require analysis-suitability for the optimal convergence rate, unlike the AS- $G^1$  construction. This  
 406 feature makes the method applicable to more complex geometries. When the Approximate  $C^1$   
 407 construction is applied to an analysis-suitable geometry with  $p \geq 3$  and  $r \leq p - 2$ , and the gluing  
 408 data approximation is exact, the construction becomes equivalent to the AS- $G^1$  construction.  
 409

410 Figure 5b presents a local region around and EV with valence five with line styles indicat-  
 411 ing different continuity levels on patch or element boundaries (see the caption of Fig. 5). For  
 412 the Approx.  $C^1$  construction on a fully smooth basis ( $p \geq 3$  and  $r = p - 1$ ), the interior basis  
 413 recovers full smoothness on element boundaries, hence  $C^{p-1}$  continuity. In the shaded region  
 414 around the interfaces and the EV, the continuity is locally reduced by construction of the locally  
 415 reduced continuous subspace and the approximation of the gluing data. Similar to the AS- $G^1$   
 416 construction, the continuity on the EV is  $C^2$  by construction and the element boundaries are  $C^1$   
 417 approximately.  
 418

419 In sum, the core ideas behind the Approx.  $C^1$  construction are as follows:

- 420 • **Degree, regularity, continuity**  
 421 The spline space is approximately  $C^1$  and fully  $C^1$  in the limit of refinement. This makes  
 422 the spline space suitable to solve fourth-order problems. Contrary to the AS- $G^1$  construc-  
 423 tion, the spline space approximates the gluing data, allowing maximal smoothness in the  
 424 interior space ( $r = p - 1$ ) for degrees  $p \geq 3$ .
- 425 • **Limitations on construction**  
 426 The space can be constructed on fully unstructured quadrilateral meshes with both interior

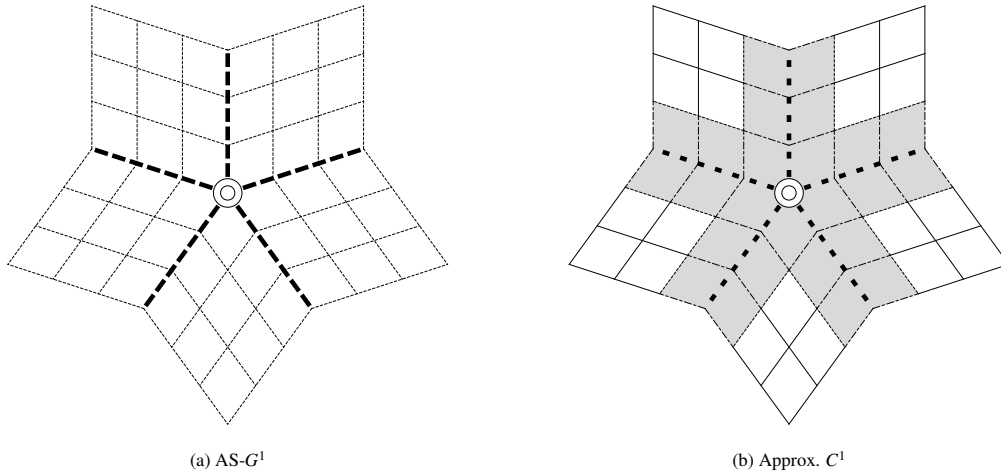


Figure 5: Schematic representation of the continuity across element boundaries and patch interfaces for the (a) AS- $G^1$  construction, (b) Approx.  $C^1$  constructions. Thin lines indicate element boundaries and thick lines indicate patch interfaces. Solid lines represent  $C^{p-1}$  continuity, dashed lines represent  $C^{p-2}$  continuity, thick dashed lines represent  $C^1$  interfaces and loosely dashed lines represent approximate  $C^1$  interfaces. A double lined circle represent a  $C^2$  continuous vertex, a filled circle represent a singular vertex and a white filled circled with a single line represents a  $C^1$  continuous vertex. The gray shaded area for the Approx.  $C^1$  represents local reduced continuity.

427 and boundary extraordinary vertices. The construction of the basis functions is independent of the location or valence of the vertices. Contrary to AS- $G^1$  the analysis-suitability condition is not needed. However, the construction requires a  $G^1$  condition at the interfaces of surfaces.

431 • **Nestedness**

432 The spline spaces are not nested.

433 • **Refinement procedure**

434 Refinement procedure is standard since the parameterization does not change.

435 **3.3. D-patch**

436 The relative ease of imposing parametric smoothness for splines has led to the development of degenerate Bezier patches, or D-patches [89], which can be used to build  $C^1$  smooth splines on unstructured quadrilateral meshes with no boundary extraordinary vertices. The constructions can be formulated for splines of any bi-degree [75], and there are no restrictions on their smoothness in the locally-structured regions of the mesh. In the locally-unstructured regions of the mesh (i.e., in a neighbourhood of an extraordinary vertex), the splines are  $C^1$  smooth and first-order degenerate. Note that this degeneracy means that the spline spaces are not necessarily  $H^2$ -conforming, but numerical evidence shows that they can still be used to solve fourth-order problems.

445  
446 Specifically, imposition of strong  $C^1$  smoothness around an extraordinary vertex requires that the splines vanish up to first order at the extraordinary vertex. This degeneracy trivially implies  
447

448 matching first derivatives at the extraordinary vertex (since all of them vanish) but does not im-  
 449 ply  $C^1$  smoothness of the resulting spline functions and the geometries built using them. As  
 450 shown in [89], additional conditions can be imposed upon certain higher-order mixed derivatives  
 451 to ensure this desired  $C^1$  smoothness. Furthermore, the effect of these additional constraints can  
 452 be localised to a neighbourhood of the extraordinary vertex by imposing them on a subdivided  
 453 representation of the splines [90]. This means that a patch-based representation of  $C^1$  D-patch  
 454 splines takes functions that are in  $\mathcal{S}(\mathbf{p}, \mathbf{r}, \mathbf{h}/2)$  on each patch, where almost all basis functions are  
 455 in  $\mathcal{S}(\mathbf{p}, \mathbf{r}, \mathbf{h})$ , except a few basis functions supported in a neighbourhood of extraordinary points  
 456 (the number of basis functions depends on the valence).

457  
 458 The D-patch construction allows for nested refinements of the spline spaces [89]. If different  
 459 orders of smoothness are being imposed in locally-structured and locally-unstructured regions of  
 460 the mesh, then nested refinements produce spline spaces with a higher number of basis functions  
 461 supported in the vicinity of extraordinary points (the number depends on the refinement-level),  
 462 see [10] for instance. On the other hand, a patch-based approach allows for a simpler implemen-  
 463 tation by limiting the smoothness across patch interfaces to  $C^1$ ; the smoothness in patch-interiors  
 464 can still be arbitrarily chosen. However, special care should be taken when using D-patches with  
 465 nested refinements – the degeneracy of the splines near extraordinary vertices means that, with  
 466 mesh refinements, the shape regularity of the mesh starts to worsen with refinements and the  
 467 finite element matrices become very ill-conditioned.

468  
 469 In sum, the core ideas behind the D-patch spline construction are the following:

- 470 • **Degree, regularity, continuity**  
 471 The spline space is fully  $C^1$ . In general, the degeneracy of derivatives means that the  
 472 spaces are  $H^2$ -nonconforming, however numerical evidence supports their use in solving  
 473 fourth-order problems. The construction can be formulated for splines of any degree and  
 474 the smoothness away from extraordinary vertices can be chosen arbitrarily.
- 475 • **Limitations on construction**  
 476 The space can be constructed on unstructured quadrilateral meshes with no boundary ex-  
 477 traordinary vertices.
- 478 • **Nestedness**  
 479 The spline spaces can be refined in a nested manner, however the resulting mesh have poor  
 480 shape regularity and the corresponding finite element matrices may be very ill-conditioned.
- 481 • **Refinement procedure**  
 482 Refinement procedures can be derived from standard B-spline knot insertion.

### 483 3.4. Almost $C^1$

484 Almost- $C^1$  splines are defined on a general, conforming quadrilateral mesh. They are piece-  
 485 wise biquadratic and possess mixed smoothness, i.e., they are  $C^1$  in regular regions, while the  
 486 smoothness near extraordinary vertices, i.e., vertices with valence different from four, is reduced.  
 487 To be precise, they are  $C^1$  smooth at all vertices (including extraordinary vertices) and across all  
 488 edges except for the ones emanating from an extraordinary vertex. Moreover, while they are de-  
 489 fined to be biquadratic on all regular elements, they are piece-wise biquadratic splines (with one  
 490 inner knot in each direction) on all elements that are neighboring an extraordinary vertex. Details

491 can be found in [11]. As a consequence, a patch based representation of Almost- $C^1$  splines takes  
 492 functions that are in  $\mathcal{S}(\mathbf{2}, \mathbf{1}, \mathbf{h}/2)$  on each patch, where almost all basis functions are in  $\mathcal{S}(\mathbf{2}, \mathbf{1}, \mathbf{h})$ ,  
 493 except a few basis functions supported in a 1-ring neighbourhood of extraordinary points (the  
 494 number depends on the valence).

495  
 496 A central feature of Almost- $C^1$  splines is the mixed smoothness imposition described above.  
 497 In particular, this choice of mixed smoothness only depends on the current refinement level of  
 498 the mesh. That is, standard  $C^1$ -smoothness is enforced across all edges at the current refinement  
 499 level except the ones that are incident upon extraordinary vertices, where only  $C^0$  smoothness is  
 500 enforced. Additionally, these smoothness conditions are combined with  $G^1$  smoothness imposi-  
 501 tion at each extraordinary vertex. This means that almost- $C^1$  splines do not yield nested spaces  
 502 when refining. As a result, the refinement process essentially amounts to a projection of coarse  
 503 Almost- $C^1$  splines onto the refined Almost- $C^1$  spline space. This projection can be chosen in  
 504 many different ways and can have a significant impact on the limit surface description as well as  
 505 isogeometric simulations using these spaces. In [11] a smoothing and refinement procedure is  
 506 proposed that results in a  $C^1$ -smooth limit surface for sufficiently regular input data.

507  
 508 Let us briefly summarize the refinement procedure here. We assume that we are given a quad  
 509 mesh and associate a control point with each face of the mesh. The initial smoothing step guaran-  
 510 tees that all control points associated to the one ring around an extraordinary vertex are coplanar.  
 511 Having given such an initial control point grid, we then refine the geometry using explicit sub-  
 512 division rules as specified in [11, 105]. The rules are the same as for quadratic tensor-product  
 513 B-splines in regular regions and maintain the coplanarity near extraordinary vertices.

514  
 515 In sum, the core ideas behind the Almost- $C^1$  spline construction are the following:

- 516 • **Degree, regularity, continuity**  
 517 The spline space locally reproduces biquadratic polynomials and it is sufficiently smooth  
 518 to be able to solve fourth order problems.
- 519 • **Limitations on construction**  
 520 The splines can be constructed on fully unstructured quadrilateral meshes, in particular,  
 521 those that contain both interior and boundary extraordinary vertices.
- 522 • **Nestedness**  
 523 Since the spaces are not nested, the convergence behavior of Almost- $C^1$  splines depends  
 524 on how the geometry parameterization is refined.
- 525 • **Refinement procedure**  
 526 An initial geometry and a refinement procedure can be constructed in such a way, that the  
 527 limit geometry parameterization is normal continuous everywhere.

528 Thus, the concept introduced in [11] is quite flexible, since the initial smoothing procedure  
 529 and the refinement procedure are not unique and can be tailored to the needs coming from geo-  
 530 metric modeling, e.g., one may want to reproduce Doo-Sabin subdivision surfaces, thus having  
 531 to modify the subdivision rule for refinement accordingly. The spline space that is introduced  
 532 on each refinement level can be seen as a simple hole-filling construction, which is sufficient for  
 533 numerical analysis.

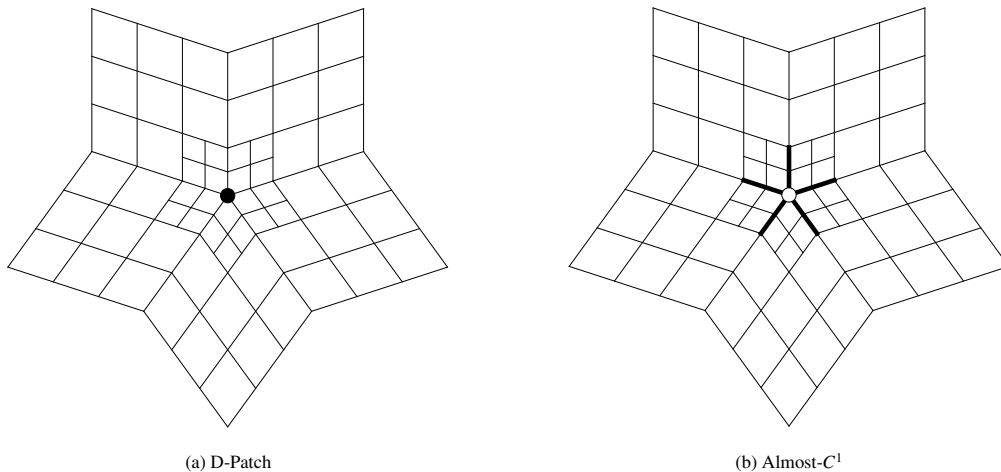


Figure 6: Schematic representation of the continuity across element boundaries and patch interfaces for the (a) D-Patch and (b) Almost- $C^1$ . Line styles are as in Fig. 5.

### 534 3.5. Conclusions

535 In this section, a summary of the construction and the properties of the analysis-suitable  $G^1$   
 536 (AS- $G^1$ ), the approximate  $C^1$  (Approx.  $C^1$ ), the degenerate patches (D-patch) and the Almost- $C^1$   
 537 methods have been provided, referring to the relevant publications for the mathematical details.  
 538 For each method, comments have been provided on the degree, regularity and continuity of the  
 539 space, on the limitations of the construction in terms of the quadrilateral mesh, on nestedness for  
 540 refinement and on the refinement procedure itself. In addition, Figs. 5 and 6 provides detailed  
 541 information on the local continuity of the constructions around an extraordinary vertex.

542  
 543 The aim of the qualitative analysis of the methods in this paper is to provide a comparison  
 544 of a set of properties and requirements of each method and their implications on their applica-  
 545 bility. While the subsections presented before provide a brief description of the properties of the  
 546 methods and the reason behind these properties and requirements, Table 1 provides a side-by-  
 547 side comparison of each method based on the subsections before. In particular, the table lists the  
 548 (i,ii) requirements on degree and regularity for the constructions, iii geometrical or topological  
 549 limitations if applicable, (iv,v) the continuity of the constructed bases in the interior and on the  
 550 interfaces and element boundaries and vi nestedness of the constructed basis.

551  
 552 Following from Table 1, the requirements for construction of the unstructured spline bases  
 553 are summarized in Fig. 7 as pre-processing conditions that have to be satisfied for each unstruc-  
 554 tured spline construction in the process depicted in Fig. 2. The degree and regularity conditions  
 555 (cf. i,ii in Table 1) must be satisfied for each construction, e.g. by performing projections on  
 556 suitable spline spaces or by knot insertion routines. Furthermore, the geometric or topological  
 557 limitations (cf. iii in Table 1) impose additional constraints that the geometry must satisfy.

558

Table 1: Summary of the requirements for the construction and the properties for each of the considered bases. The construction requirements include the degree and regularity of the basis used for construction as well as geometrical or topological properties of the input geometry. The properties include the continuity on interfaces, vertices and in the interior of the unstructured spline construction, as well as the nestedness property.

Requirements	AS- $G^1$	Approx. $C^1$	D-Patch	Almost- $C^1$
(i) Degree	$p \geq 3$	$p \geq 3$	$p \geq 3$	$p = 2$
(ii) Regularity	$r \leq p - 2$	$r \leq p - 1$	$r \leq p - 1$	$r = 1$
(v) Geometrical / topological limitations	Analysis-suitability	$G^2$ continuity	BEVs: $v \leq 3$ , $C^1$ continuity	$C^1$ continuity
Properties	AS- $G^1$	Approx. $C^1$	D-Patch	Almost- $C^1$
(iii) Interface & Vertex Continuity	$C^1$	$C^1$ in the limit	$C^1$	$C^1$ in the limit
(iv) Interior continuity	$C^{p-2}$	$C^{p-1}$	$C^{p-1}$	$C^1$
(vi) Nestedness	Yes	No	Yes	No

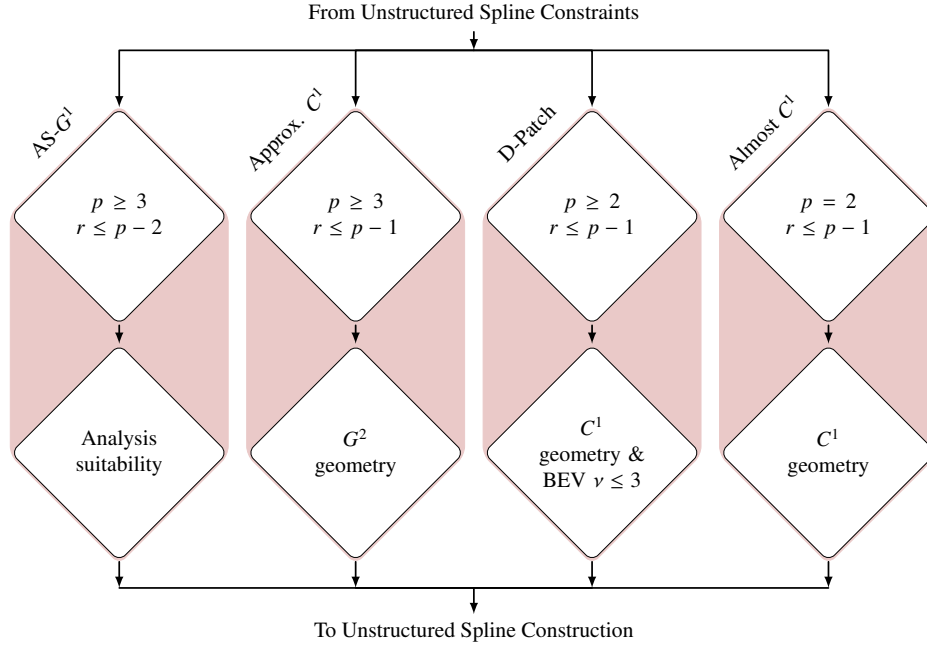


Figure 7: Inside the *unstructured spline pre-processing* block from Fig. 2. The unstructured spline requirements are depicted in diamond-shaped blocks for methods AS- $G^1$ , Approx.  $C^1$ , D-Patch and Almost  $C^1$ . The first row represents requirements on degree  $p$  and regularity  $r$ . If not satisfied, the geometry can be projected onto a space that satisfies the requirement, or degree elevation or reduction steps can be performed together with refinement operations. The second row depicts the requirements on the geometry parameterization; these blocks can be satisfied by changing the geometry.

559 **4. Quantitative comparison**

560 In this section a quantitative comparison between the methods provided in Section 3 is pro-  
561 vided. In addition, variational coupling methods are compared if applicable. The quantitative  
562 comparison is composed of various benchmark problems, each providing a different conclusion  
563 with respect to the methods considered:

564 **Biharmonic problem on a planar domain (Section 4.1)** The first example entails solving the  
565 biharmonic problem on a planar domain. The goal of this example is to assess the con-  
566 vergence properties of all considered unstructured spline constructions, hence the problem  
567 will be solved on a simple analysis-suitable geometry without EVs on the boundary, such  
568 that every method from Section 3 can be applied and compared to the manufactured solu-  
569 tion.

570 **Linear Kirchhoff–Love shell analysis on a surface (Section 4.2)** The second example entails  
571 solving the Kirchhoff–Love shell equation on curved domains. The goal of this example  
572 is to demonstrate the performance of the unstructured spline construction for simple shell  
573 problems. Therefore, comparison will be made to single-patch results and penalty coupling  
574 from [51].

575 **Spectral analysis on a planar domain (Section 4.3)** In the third example, spectral analysis of  
576 a plate equation is performed. The goal of this example is to assess the spectral properties  
577 of the unstructured spline methods compared to a variational approach and a single patch,  
578 since the spectral properties of highly continuous bases have been demonstrated to be  
579 superior over non-smooth bases [110].

580 **Modal analysis of a complex geometry (Section 4.4)** In the fourth example, a modal analysis  
581 is performed on a complex geometry extracted from a quad-mesh. The goal of this example  
582 is to demonstrate the applicability and performance of the unstructured spline methods on  
583 a large-scale, more complicated geometry.

584 **Stress analysis in a curved shell (Section 4.5)** Lastly, the fifth example involves the analysis of  
585 stress fields in shells. The goal of this example is to assess the performance of unstructured  
586 spline constructions and a penalty method when it comes to stress reconstruction in shells.  
587 For the Kirchhoff–Love shell, the stresses are obtained by taking gradients of the deformed  
588 geometry, hence of the solution. This means that for  $C^1$  bases, stresses are  $C^0$ . This might  
589 be unfavourable in engineering applications where local stress fields are of importance,  
590 e.g. fatigue analysis.

591 In all examples except the complex geometry in Section 4.4, the domain decomposition from  
592 Fig. 8 is used to decompose a simple domain into a domain with extraordinary vertices in the  
593 interior. Domains with EVs on the boundary are left out of scope, since the D-patch construction  
594 would change the outer boundaries of the domain, hence the comparison would involve a signif-  
595 icantly different geometry. Since different methods have different constraints on the degree and  
596 regularity of the basis, different combinations of the degree  $p$  and regularity  $r$  are tested through-  
597 out the benchmark problems. In Table 2 the combinations of  $p$  and  $r$  and the methods that are  
598 compared for these bases are provided. For the biharmonic problem and the spectral analysis  
599 (Sections 4.1 and 4.3) Nitsche’s method is used for comparison, see [47] for more details. When  
600 solving the Kirchhoff–Love shell equations, the penalty method is used for comparison, see [51]





Figure 8: Multi-patch decomposition of a simple domain into six patches. The domain has two EVs in the interior (valence 3 and 5) and no boundary EVs.

Table 2: Degree  $p$  and regularity  $r$  constraints for each considered method from Section 3, see Table 1.

	$p = 2, r = 1$	$p = 3, r = 1$	$p = 3, r = 2$
D-patch	★	★	★
Almost- $C^1$	★		
Approx. $C^1$		★	★
AS- $G^1$		★	
Nitsche/Penalty	★	★	★

601 for more details. In all examples, Dirichlet boundary conditions are applied at the control points  
 602 and clamped boundary conditions are applied weakly as in [51]. All results are obtained using  
 603 the Geometry + Simulation modules [111, 112] and will be published in a separate publication.

604

605 As discussed in Section 3, the D-patch and Almost- $C^1$  constructions involve a pre-smoothing  
 606 of the geometry. In case of mesh convergence results, refinements can be performed in different  
 607 ways. On the one hand, the original geometry can be refined and a new construction with a new  
 608 geometry approximation can be performed. On the other hand, the geometry resulting from the  
 609 construction in the first refinement level can be refined in a nested way, such that the geometry  
 610 does not change after the first mesh. In the quantitative comparison, all refinements are performed  
 611 in a nested way, unless specified otherwise.

#### 612 4.1. Biharmonic equation on a planar domain

613 The first benchmark entails the biharmonic equation on a planar domain. The purpose of this  
 614 example is to assess the convergence properties of the unstructured spline methods described in  
 615 Section 3. We mainly follow the structure of [47]. The biharmonic equation is solved on a unit  
 616 square  $\Omega = [0, 1]^2$  with the patch segmentation from Fig. 8. The biharmonic equation is defined  
 617 by

$$\Delta^2 \varphi = f. \quad (1)$$

618 In the present example, convergence is analysed with respect to a manufactured solution

$$\tilde{\varphi}(x_1, x_2) = (\cos(4\pi x_1) - 1)(\cos(4\pi x_2) - 1), \quad (2)$$

619 such that the right-hand-side function becomes:

$$f(x_1, x_2) = 256\pi^4(4 \cos(4\pi x) \cos(4\pi y) - \cos(4\pi x) - \cos(4\pi y)) \quad (3)$$

620 Furthermore, on all boundaries of the domain, the manufactured solution and its derivatives are  
621 imposed as Dirichlet and Neumann boundary conditions, respectively:

$$\left. \begin{aligned} \varphi &= \tilde{\varphi}(x_1, x_2) \\ \partial_{\mathbf{n}}\varphi &= \partial_{\mathbf{n}}\tilde{\varphi} \end{aligned} \right\} \text{on } \Gamma, \quad (4)$$

622 where  $\Gamma = \partial\Omega$ ,  $\mathbf{n}$  is the unit outward normal vector on  $\Gamma$ . The biharmonic equation from Eq. (1)  
623 with boundary conditions Eq. (4) can be discretized by obtaining the weak formulation, see [47],  
624 inserting Eq. (4) and by defining an approximation of the solution  $\varphi$  as  $\varphi_h$ . Furthermore, a weak  
625 coupling can be established through Nitsche's method. For the mathematical details behind the  
626 discretization of the biharmonic equation and optionally adding Nitsche interface coupling terms,  
627 we refer to [9, 47]. For the D-Patch and Almost  $C^1$  constructions, the geometry is smoothed upon  
628 construction. The geometry used for evaluation of the weak formulation is constructed by using  
629 an  $L_2$ -projection of the geometry from the coarsest space which is projected onto the smooth  
630 basis of each refinement level. For the D-Patch, the non-negative smoothness matrix for vertex  
631 smoothing is used. Although this matrix produces non-nested meshes, it provides the highest  
632 rates of convergence. Furthermore, the factor  $\beta$  (cf. [10, sec. 5.1]) is chosen as  $\beta = 0.4$  as used  
633 by [10], or  $\beta = 1.2$ , and halved in each refinement level.

634  
635 To evaluate the unstructured spline constructions from Section 3, the numerical approxima-  
636 tion  $\varphi_h$  is compared to the manufactured solution  $\tilde{\varphi}$  in the  $L^2$ -,  $H^1$ - and  $H^2$ -norms on the multi-  
637 patch segmentation from Fig. 8. The bi-linear segmentation is refined and degree elevated until  
638 the desired degree  $p$  and regularity  $r$  from Table 2 are obtained. In addition, a Nitsche coupling  
639 of the patches is employed for comparison.

640  
641 The results for the comparison are presented in Fig. 9. For degree  $p = 2$  and regularity  
642  $r = 1$  the Almost- $C^1$ , D-patch and Nitsche coupling methods are compared. As expected, the  
643 results show consistency between the Almost- $C^1$ , D-patch and Nitsche's method with expected  
644 convergence. The results also show a slight dependency on the factor  $\beta$  for the D-Patch. For  
645 degree  $p = 3$  and regularity  $r = 1$ , the Approx.  $C^1$ , AS- $G^1$ , D-patch and Nitsche's method can be  
646 compared. The results of the Approx.  $C^1$  and AS- $G^1$  are exactly the same, since the original ge-  
647 ometry is analysis-suitable and contains only bi-linear patches. Then applying the Approx.  $C^1$  to  
648 an analysis-suitable geometry with regularity  $p - 2$ , the approximate gluing data becomes exact,  
649 hence the same as in the AS- $G^1$  construction. The D-patch in this case shows better convergence  
650 of the  $L_2$ ,  $H_1$  and  $H_2$  errors for  $\beta = 1.2$  than for  $\beta = 0.4$ . Though, for both choices of  $\beta$ , the  
651 convergence is sub-optimal, as was observed in the work by [91]. Furthermore, the  $L_2$ -norm in-  
652 creases at the last point of the D-Patch results, due to ill-conditioning of the system of equations.  
653 Lastly, for degree  $p = 3$  and regularity  $r = 2$  the Approx.  $C^1$ , D-patch and Nitsche's method are  
654 compared. The observations are as for the  $p = 3$ ,  $r = 1$  case.

655

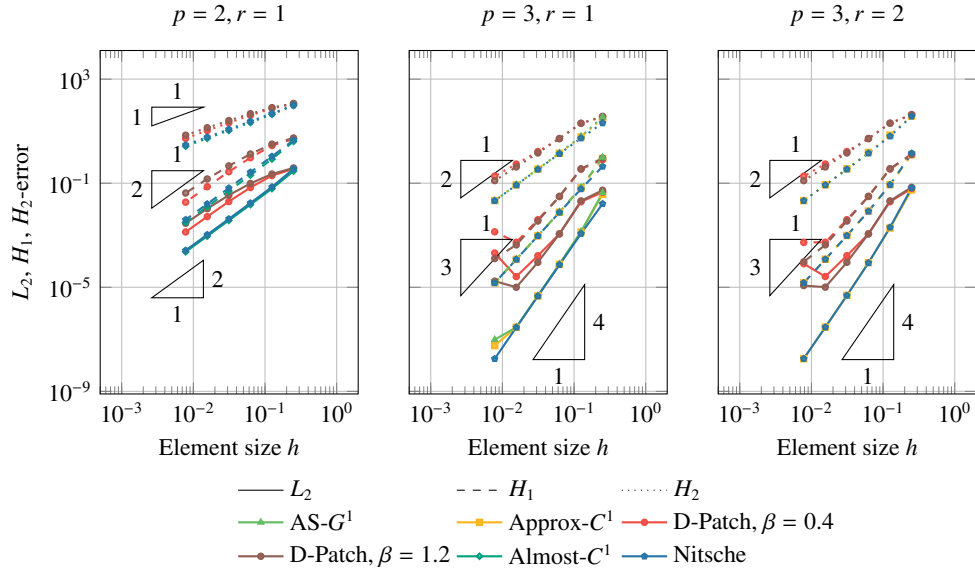


Figure 9: Errors for the AS- $G^1$ , Approx- $C^1$ , D-Patch and Almost- $C^1$  construction for the biharmonic problem on the domain in Fig. 8. The  $L_2$ ,  $H_1$  and  $H_2$  errors with respect to the analytical solution are plotted with different line styles in the top row. Furthermore, all results are plotted against the element size  $h$  and the expected convergence rates are given by the triangles.

656 Overall, the results show expected convergence behaviour for all considered spline construc-  
 657 tions compared to theoretical results and compared to a Nitsche coupling method. However, the  
 658 D-Patch method does not converge for very fine meshes, due to ill-conditioning of the system  
 659 matrix.

#### 660 4.2. Linear Kirchhoff–Love shell analysis on a surface

661 We solve the linear Kirchhoff–Love shell equations on two geometries to demonstrate the  
 662 convergence behaviour of the methods on curved surfaces. To this end, two benchmark examples  
 663 are considered. Firstly, a hyperbolic paraboloid surface is constructed with shape, inspired by  
 664 [8]:

$$\mathbf{r}(\xi_1, \xi_2) = \begin{bmatrix} \xi_1 & \xi_2 & \xi_1^2 - \xi_2^2 \end{bmatrix} \quad (5)$$

665 The left-side of the hyperbolic paraboloid is clamped ( $\mathbf{u} = \mathbf{0}$ ) and the other sides are free. Fur-  
 666 thermore, a distributed load with magnitude  $8000t$  is applied with  $t$  the thickness, see Fig. 10.  
 667 Secondly, an elliptic paraboloid shaped-domain is modelled, with equation

$$\mathbf{r}(\xi_1, \xi_2) = \begin{bmatrix} \xi_1 & \xi_2 & 1 - 2(\xi_1^2 + \xi_2^2) \end{bmatrix} \quad (6)$$

668 For this shape, a point load with magnitude  $10^8 t$  is applied in the middle of the domain. The  
 669 corners of the domain are only fixed in vertical  $z$  direction to allow sliding in the  $xy$ -plane. One  
 670 corner is fixed in all directions to create a well-posed problem. For both hyperbolic paraboloid  
 671 (Fig. 10) and elliptic paraboloid (Fig. 11) the multi-patch segmentation from Fig. 8 is used. In  
 672 both cases, the shells are modelled with a thickness of  $t = 0.01$  [mm] and with a Saint-Venant

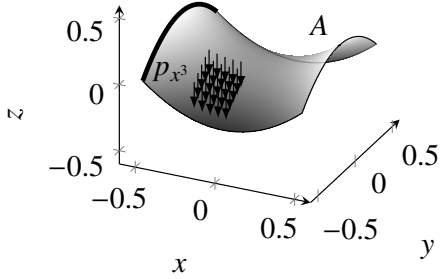


Figure 10: Hyperbolic paraboloid shell geometry with coordinates  $\mathbf{r}(\xi_1, \xi_2) = [\xi_1 \quad \xi_2 \quad \xi_1^2 - \xi_2^2]$ ,  $\xi_1, \xi_2 \in [-1/2, 1/2]$ . The left-edge of the hyperbolic paraboloid is clamped, i.e. the displacements and rotations are zero ( $\mathbf{u} = \mathbf{0}$  and  $\frac{\partial u_z}{\partial x} = 0$ ).

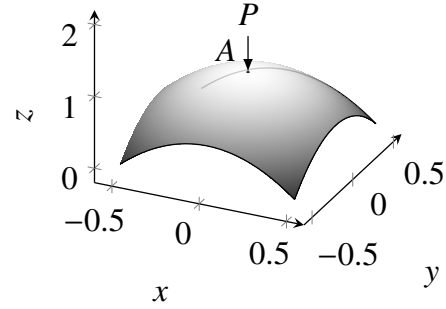


Figure 11: Elliptic paraboloid shell geometry with coordinates  $\mathbf{r}(\xi_1, \xi_2) = [\xi_1 \quad \xi_2 \quad 1 - 2(\xi_1^2 + \xi_2^2)]$ ,  $\xi_1, \xi_2 \in [-1/2, 1/2]$ . On the corners of the domain, the vertical displacements are set to zero  $u_z = 0$  and one corner is fixed in-plane as well. Furthermore, a point load with magnitude  $P = 10^8 t$  is applied in the middle of the geometry.

673 Kirchhoff material with Young's modulus  $E = 200$  [GPa] and Poisson's ratio  $\nu = 0.3$  [-]. The  
 674 refinement procedure as described in Section 4.1 is used for the D-Patch and Almost- $C^1$   
 675 constructions.

676  
 677 The results of both analyses are given in Figs. 12 and 13. Here, different unstructured spline  
 678 constructions are tested on patch-bases with different degrees and regularities, as reported in Ta-  
 679 ble 2. For each combination of degree  $p$  and regularity  $r$ , the energy norm  $W_{\text{int}}^h = \frac{1}{2} \mathbf{u}_h^\top K_h \mathbf{u}_h$   
 680 is plotted against the number of degrees of freedom, with  $\mathbf{u}_h$  the discrete displacement vector and  
 681  $K_h$  the discrete linear stiffness matrix. From the results in Figs. 12 and 13, a few observations can  
 682 be made. Firstly, the Approx.  $C^1$  and AS- $G^1$  methods show slow convergence on the hyperbolic  
 683 paraboloid geometry, while the convergence on the elliptic paraboloid geometry is similar to the  
 684 single-patch convergence. The slow convergence for the hyperbolic paraboloid shell is also ob-  
 685 served in [8]. Since the results of the same constructions on the elliptic paraboloid geometries  
 686 do not show slower convergence, the slow convergence is hypothetically a result of the double  
 687 curvature with different signs of the shell. Secondly, the D-Patch and Approx.  $C^1$  show com-  
 688 parable convergence to the penalty method on both geometries, which is slightly slower than the  
 689 convergence of the single-patch results. This is explained by the fact that the degrees of freedom  
 690 are more optimally allocated for the single-patch parameterization. Lastly, the results obtained  
 691 by the penalty method for different penalty parameters  $\alpha$  show convergence with a rate similar to  
 692 the D-Patch and Almost- $C^1$  methods for penalty parameters  $\alpha \in \{1, 10\}$ . For  $\alpha = 100$  the penalty  
 693 method is still converging to the same solution, but convergence starts after a few refinement  
 694 steps.

### 695 4.3. Spectral analysis on a planar domain

696 In this example, the spectral properties of the unstructured spline constructions on a multi-  
 697 patch domain are considered. From [4] it is known that isogeometric analysis has the advan-

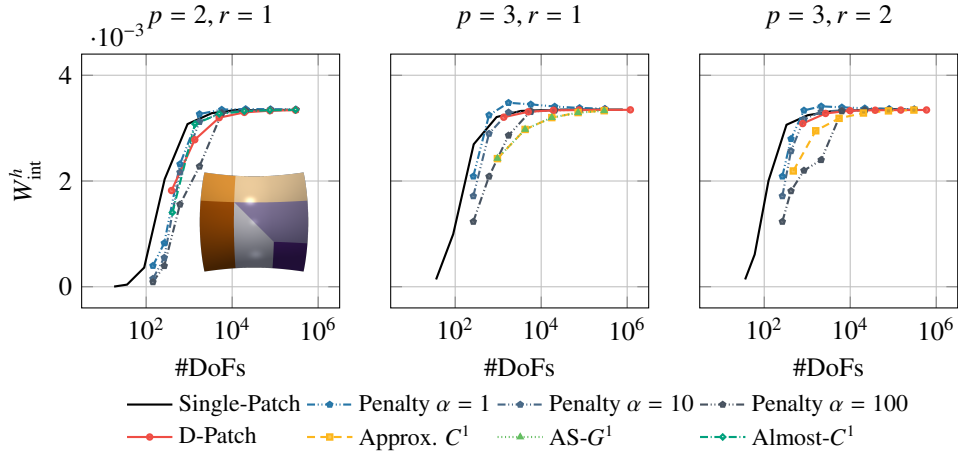


Figure 12: Bending energy norm  $W_{\text{int}}^h = \frac{1}{2} \mathbf{u}_h^\top K_h \mathbf{u}_h$  for the hyperboloid geometry from Fig. 10 with a patch segmentation as in Fig. 8. The results are presented for different combinations of the degree  $p$  and regularity  $r$  for all unstructured spline constructions. In addition, the results for a penalty method with parameter  $\alpha \in \{1, 10, 100\}$  are provided for comparison.

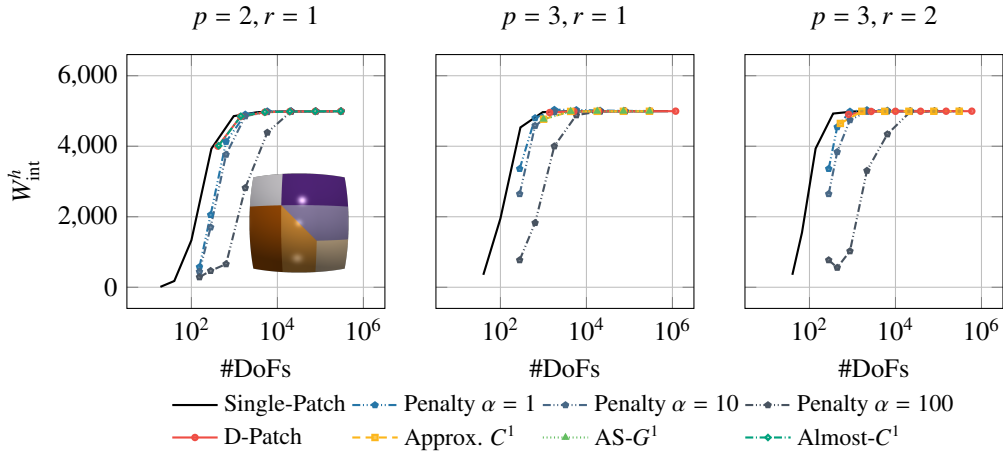


Figure 13: Bending energy norm  $W_{\text{int}}^h = \frac{1}{2} \mathbf{u}_h^\top K_h \mathbf{u}_h$  for the paraboloid geometry from Fig. 11 with a patch segmentation as in Fig. 8. The results are presented for different combinations of the degree  $p$  and regularity  $r$  for all unstructured spline constructions. In addition, the results for a penalty method with parameter  $\alpha \in \{1, 10, 100\}$  are provided for comparison.

698 tage over  $C^0$  Finite Element Analysis with respect to spectra for eigenvalue problems. Smooth  
699 isogeometric discretization provide converging spectra with spline degree  $p$ , whereas the spec-  
700 tra obtained by  $C^0$  FEA diverge with  $p$  and typically have optical branches. Similarly, when  
701 patches with  $C^0$  continuity are considered, optical branches are introduced and the accuracy of  
702 the spectral approximation decreases [113]. In this benchmark problem, we compare the basis  
703 constructions from Table 2 on Fig. 8 on their spectral properties. For Nitsche’s method, we use  
704 different values for the coupling parameter to assess its influence on the spectrum.

705  
706 For the problem at hand, we consider a unit-square domain with parametric lay-out from  
707 Fig. 8 for simplicity. We consider modal analysis using the plate equation. The stiffness operator  
708 of the free vibration plate equation is similar to the biharmonic equation from Eq. (1), and the  
709 inertia is included on the right-hand-side:

$$D\Delta^2 w = -\rho t \frac{\partial^2 w}{\partial \tau^2} \quad (7)$$

710 Assuming that  $w(x, y, \tau)$  is harmonic, i.e.  $w(x, y, \tau) = \hat{w}(x, y) \exp\{i\omega\tau\}$  with  $\omega$  a frequency, the  
711 equation simplifies to

$$D\Delta^2 \hat{w} = \omega^2 \frac{\partial^2 \hat{w}}{\partial \tau^2}. \quad (8)$$

712 Here,  $D = Et^3/(12(1 - \nu^2))$  is the flexural rigidity of the plate with  $E = 10^5$  [Pa] the Young’s  
713 modulus of the plate,  $t = 10^{-2}$  [m] the thickness and  $\nu = 0.2$  [-] the Poisson’s ratio. Furthermore,  
714  $\rho = 10^5$  [kg] is the material density. Equation (8) is a generalized eigenvalue problem with  
715 eigenpairs  $(\omega_i, v_i)$  where  $\omega_i$  is the  $i^{\text{th}}$  eigenfrequency and  $v_i$  the  $i^{\text{th}}$  mode shape. The mode shape  
716 for a simply supported unit plate with  $n \times m$  half-waves is given by

$$v_{nm}(x, y) = \sin(n\pi x) \sin(m\pi y) \quad (9)$$

717 with corresponding eigenfrequency

$$\omega_{nm} = (n^2 + m^2)\pi^2 \sqrt{\frac{D}{\rho t}}. \quad (10)$$

718 In addition, the numerical solution to Eq. (8) is obtained by solving the following generalized  
719 eigenvalue problem

$$D \int_{\Omega} \Delta w \Delta \varphi \, d\Omega = \omega^2 \rho t \int_{\Omega} u \varphi \, d\Omega \quad (11)$$

720 With  $\varphi$  a test function, see Section 4.1. In further representation of the solutions, we employ the  
721 index  $i$  such that  $\omega_i < \omega_{i+1}$  and we use the subscript  $h$  for numerically obtained solutions.

722  
723 Figure 14 presents the spectra for different degrees, regularities and for different methods.  
724 Here, the vertical axis represents the ratio of the numerically obtained eigenfrequency over the  
725 analytical eigenfrequency with index  $i$ , thus  $\omega_{h,i}/\omega_i$ . The horizontal axis represents the fraction  
726 of the eigenfrequency index  $i$  over the total number of eigenmodes. The total number of eigen-  
727 modes is equal to the number of degrees of freedom in the system. The results are presented for  
728 the degrees and regularities as in Table 2.

729

730 Firstly, the  $p = 2, r = 1$  plot shows that Nitsche's method oscillates for all considered values  
731 of the penalty parameter. Furthermore, in the part where it is not oscillating, the ratio  $\omega_{i,h}/\omega_i$  is  
732 higher than for the D-patch and Almost- $C^1$  method. Additionally, the D-patch and Almost- $C^1$   
733 methods show a significant difference with respect to the single patch result, which is due to the  
734 non-Cartesian multi-patch segmentation of Fig. 8 and the fact that the analytical mode shapes are  
735 Cartesian. For the  $p = 3, r = 1$  and  $p = 3, r = 2$  bases similar conclusions can be drawn. Al-  
736 though for the  $p = 3, r = 1$  case the Approx.  $C^1$  method seems worse than the D-patch method,  
737 the opposite is true for  $p = 3, r = 2$ . Hence, it can be concluded that no method outperforms  
738 another, but that all unstructured spline constructions perform better than Nitsche's method.  
739

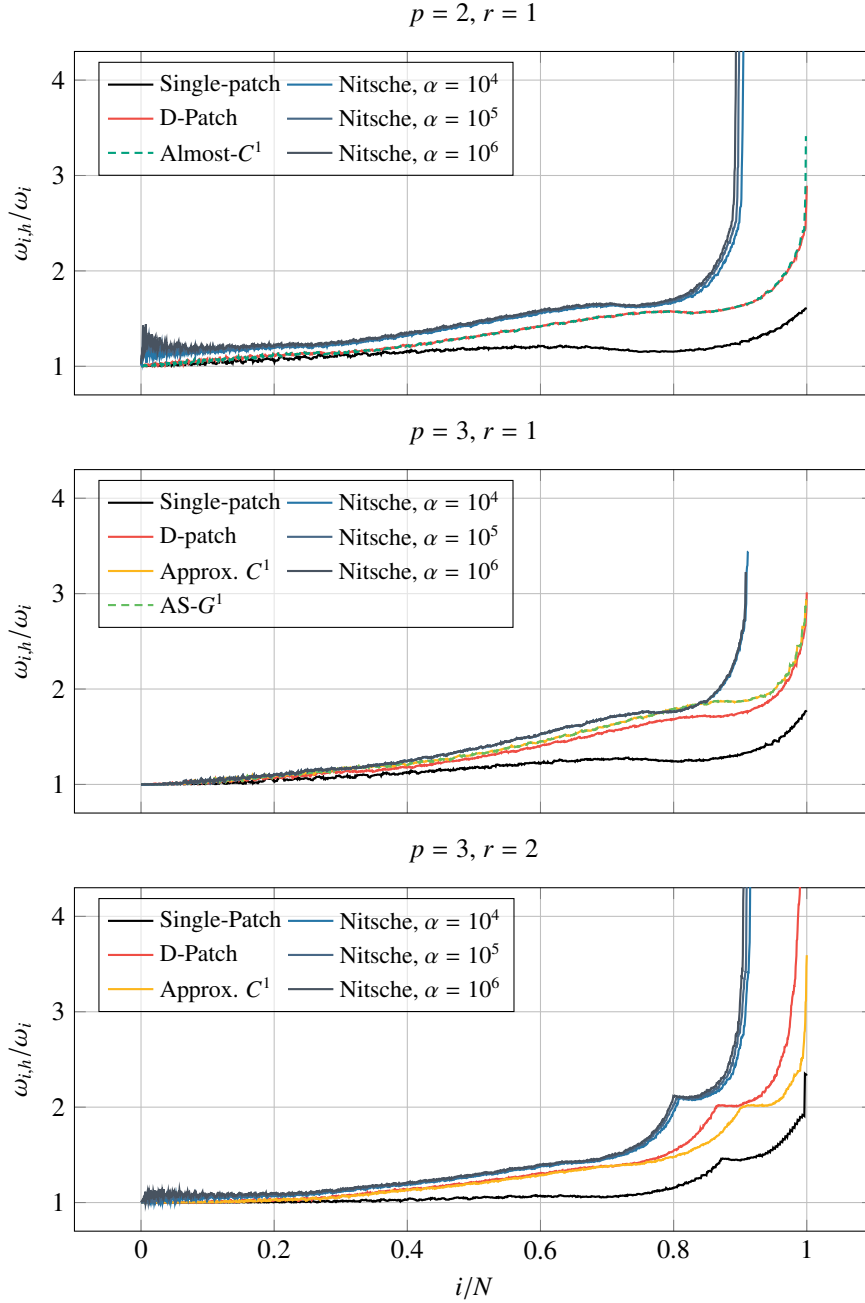


Figure 14: Eigenvalue spectra for the biharmonic eigenvalue problem on the domain from Fig. 8. The horizontal axes depict the eigenvalue index  $i$  over the total number of eigenvalues  $N$ . The vertical axes represent the numerical eigenvalue  $\omega_{i,h}$  over the analytical eigenvalue  $\omega_i$ , both with index  $i$ . The results are plotted for different combinations of the degree  $p$  and regularity  $r$  of the basis. The results for a Nitsche method are given for different penalty parameters  $\alpha$ .



740 *4.4. Modal analysis of a complex geometry*

741 The next example for the quantitative analysis in this paper involves the modal analysis on  
 742 a larger-scale complex geometry, depicted in Fig. 15a. The goal of this example is to show the  
 743 usability of the considered constructions on an off-the-shelf industrial geometry. The geometry  
 744 is represented as a mesh consisting of 15895 vertices, 31086 edges and 62172 faces. This ge-  
 745 ometry is converted to bi-linear patches using the procedure discussed in Fig. 4 in Section 3.  
 746 The interface and boundary curves of the patches are given in Fig. 15b and the final multi-patch  
 747 object is given in Fig. 15c. The latter has 3 EVs of valence 3, 10 EVs of valence 5 and 16 bEVs.  
 748 Moreover, the material parameters specified for a steel material. That is, the density of the mate-  
 749 rial is  $\rho = 7850 \cdot 10^{-6}$  [tonnes/mm<sup>3</sup>], the shell thickness is  $t = 10$  [mm], the Young's modulus is  
 750  $E = 210 \cdot 10^3$  [MPa] and the Poisson's ratio is  $\nu = 0.3$  [-]. All the sides of the geometry are kept  
 751 free, meaning that the modal analysis results will consist of six modes with zero eigenfrequen-  
 752 cies: the rigid body modes. In the sequel, we list the results for deformation modes only.

753  
 754 After the creation of the linear multi-patch object,  $h$ -,  $p$ - and  $k$ -refinement steps can be per-  
 755 formed to construct a multi-basis corresponding to the patch lay-out on which unstructured  
 756 splines can be constructed. For the Almost- $C^1$  and D-Patch constructions, the bases are con-  
 757 structed by refining and elevating the initial linear basis up to the desired degree and regularity,  
 758 after which the the Almost- $C^1$  and D-Patch basis and geometry are computed. An Almost- $C^1$   
 759 geometry is provided in Fig. 15c.

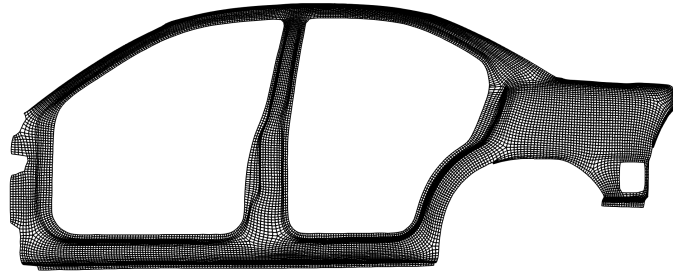
760  
 761 The AS- $G^1$  construction requires an analysis-suitable geometry, which can be constructed  
 762 following [8], which is based on the planar construction developed in [85]. However, the ge-  
 763 ometry from Fig. 15b is only  $C^0$ -smooth due to the original linear mesh it is constructed from.  
 764 An algorithm to automatically pre-process the geometry to obtain an analysis-suitable  $G^1$  sur-  
 765 face is not yet developed. The algorithm from [8] requires AS- $G^1$  gluing data, which cannot be  
 766 prescribed directly on a  $C^0$  surface. If the surface is not pre-processed to be AS- $G^1$ , no suitable  
 767 gluing data can be found and the basis construction is not applicable. Although the Approx.  $C^1$   
 768 construction does not require an analysis-suitable re-parameterization, it does require  $G^1$  smooth-  
 769 ness at the interfaces. If this condition is not satisfied there exists no  $C^1$  construction that can  
 770 be approximated by this method. For both methods, the required pre-processing efforts are non-  
 771 trivial or not demonstrated on industrial geometries, and therefore left out of the scope of this  
 772 paper<sup>3</sup>.

773  
 774 Furthermore, penalty methods have been used in the context of modal analysis on a 27 patch  
 775 composite wind-turbine blade in [51], where the variation of the element size of interface ele-  
 776 ments seems rather small. In the present paper, an attempt was made to apply the penalty method  
 777 on the geometry in Fig. 15c, but unidentifiable vibration modes were obtained, possibly because  
 778 of the large variation of element lengths across the interfaces of the domain, challenging the de-  
 779 termination of a suitable penalty parameter  $\alpha$ .

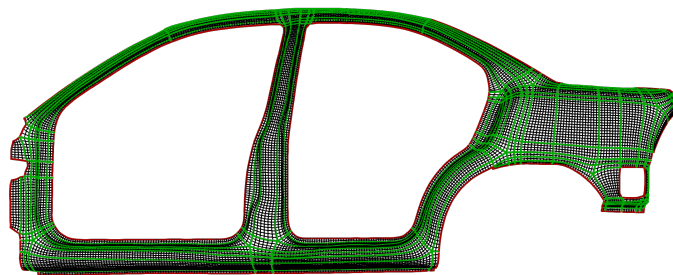
780  
 781 Table 3 presents the eigenfrequencies for the first four deformation modes of the car side  
 782 panel for the D-Patch and the Almost- $C^1$  constructions with degree  $p = 2$  and regularity  $r = 1$

---

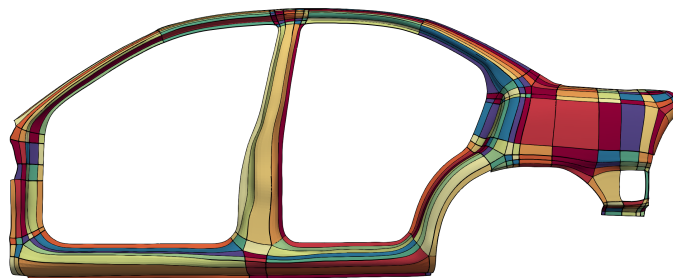
<sup>3</sup>In the case of a different starting point for this benchmark, such as a smooth mesh composed of higher-order quadri-  
 lateral elements, e.g. derived from a subdivision surface, instead of a bi-linear mesh, the pre-processing efforts required  
 for the AS- $G^1$  and Approx.  $C^1$  will be different.



(a) Original quad mesh with 15895 vertices, 31086 edges and 62172 faces.



(b) Interface (green) and boundary (red) curves.



(c) Final multi-patch segmentation with 307 patches.

Figure 15: Geometry of the side panel of a car. The original mesh (a) is traced with the procedure from Fig. 4, yielding a set of boundary and interface curves (b). From these curves, the multi-patch segmentation (c) for isogeometric analysis is constructed following Fig. 4c.

Table 3: Eigenfrequencies of the Almost- $C^1$  and D-Patch constructions for the car geometry in Fig. 15. The results of an ABAQUS FEA simulation using the S4R element are provided as a reference. The mode-shapes are plotted in Fig. 16.

Method	# DoFs	Mode 1	Mode 2	Mode 3	Mode 4	
Almost- $C^1$ , $p = 2$ , $r = 1$	13,731	15.740	25.567	43.829	56.654	
	49,758	15.762	25.564	43.429	56.778	
	189,654	15.776	25.552	43.269	56.785	
	740,814	15.774	25.531	43.177	56.746	
D-Patch, $p = 2$ , $r = 1$	49,437	15.785	25.607	43.641	56.902	
	189,333	15.780	25.561	43.323	56.807	
	740,493	15.775	25.533	43.191	56.748	
D-Patch, $p = 3$ , $r = 1$	136,839	15.749	25.593	43.348	56.786	
	630,459	15.760	25.581	43.231	56.801	
D-Patch, $p = 3$ , $r = 2$	71,760	15.771	25.539	43.224	56.744	
	226,524	15.755	25.582	43.235	56.807	
ABAQUS S4R	10mm	126,966	15.303	24.881	42.629	54.887
	5mm	440,076	15.224	24.780	42.516	54.627
	2.5mm	1,653,030	15.119	24.640	42.338	54.277

783 for the Almost- $C^1$  construction and with  $(p, r) = (2, 1)$ ,  $(p, r) = (3, 1)$  and  $(p, r) = (3, 2)$  for  
784 the D-Patch. Figure 16 provides the corresponding mode shapes on the D-Patch geometry with  
785  $p = 3$ ,  $r = 2$  and the mode shapes have been qualitatively matched to construct Table 3. From  
786 these results, it can be observed that the Almost- $C^1$  and D-Patch methods provide eigenfrequen-  
787 cies in the same range and that the eigenfrequencies are mostly converging in the second digit.  
788 Moreover, the eigenfrequencies of the D-Patch and Almost- $C^1$  methods for coarse meshes and  
789  $p = 2$ ,  $r = 1$  already provide reasonable estimates compared to higher degrees and refinements.  
790 On the other hand, the results obtained using an ABAQUS S4R element show convergence in the  
791 second digit, and slightly lower frequencies than the IGA results, possibly because the FEM uses  
792 a different geometry approximation. Overall, it can be concluded from this benchmark problem  
793 that the Almost- $C^1$  and D-Patch are more robust for industrial and large scale geometries, that  
794 are represented by at least  $C^0$ -conforming quadrilateral meshes, compared to the Approx.  $C^1$   
795 and AS- $G^1$  methods due to the pre-processing efforts required by the latter. Furthermore, these  
796 methods are parameter-free, making them robust also with respect to penalty methods.

#### 797 4.5. Stress analysis in a curved shell

798 An interesting application for smooth unstructured spline construction is for the use of thin  
799 shell analysis for engineering applications. Not only displacements (Section 4.2) or vibrations  
800 (Section 4.4) are of interest, but also stress evaluations, for example for fatigue analysis. In  
801 the last example, we demonstrate the performance of all methods in Table 2 on the evaluation  
802 of stresses in a curved Kirchhoff–Love shell. Since the Kirchhoff–Love shell formulation is  
803 displacement-based, the displacements are  $C^1$  continuous across patch interfaces for  $C^1$  con-  
804 structions. The stresses, however, are based on the gradients of the displacements, hence their  
805 continuity theoretically is  $C^0$  for a perfect  $C^1$  coupling. In this example, we elaborate on the Von  
806 Mises membrane stress field resulting from the 6-patch elliptic paraboloid from Fig. 13. The

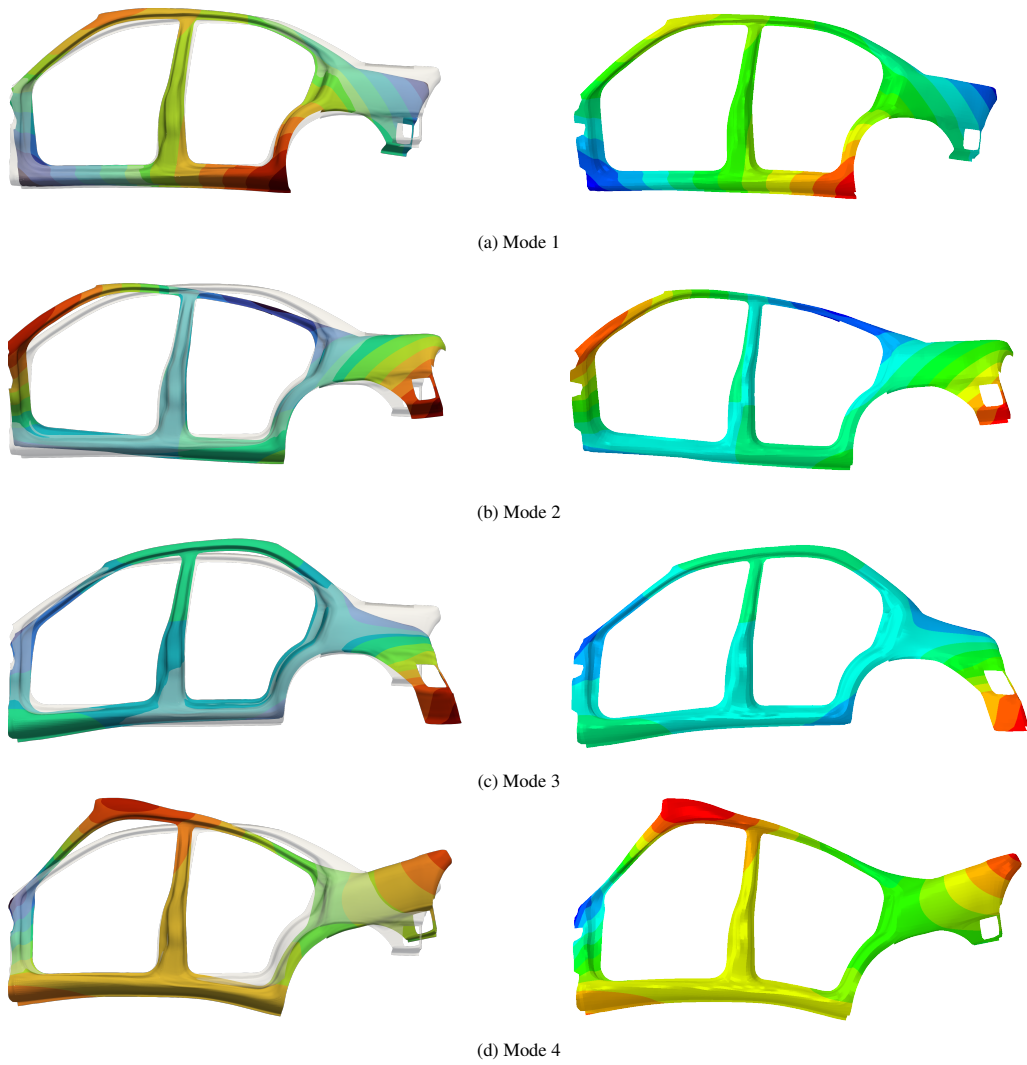


Figure 16: Out-of-plane deformations of the first four vibration modes of the side of the car from Fig. 15. The results on the left represent the results obtained by the D-Patch construction and the results on the right represent results obtained using ABAQUS (10mm). The mode shapes are all deformation modes warped by the deformation vector and plotted over the undeformed (transparent) geometry.

807 stress fields are plotted for bases with degree and regularity from Table 2 and additionally for a  
808 basis with  $p = 4$ ,  $r = 2$ . Note that the regularity  $r$  of these bases is the regularity in the patch  
809 interior.

810  
811 In Fig. 16, the stress fields for the elliptic paraboloid example from Fig. 13 are provided.  
812 From these results, it can immediately be seen that the stress field for a single patch parameter-  
813 ization with basis  $p = 2$ ,  $r = 1$  exposes the elements of the basis because of the  $C^0$  continuity  
814 across elements. Similar effects are seen for the D-patch, Almost- $C^1$  and the penalty method.  
815 Increasing the degree of the basis while keeping the regularity the same results in a  $p = 3$ ,  $r = 1$   
816 basis. The element continuity is still  $C^0$  for the stresses, but the higher continuity of the basis  
817 within the element results in a slightly improved stress field, as can be seen from the single patch,  
818 the D-patch and penalty methods. The Approx.  $C^1$  and AS- $G^1$  methods in addition show a better  
819 stress field around the EVs compared to the D-patch with only small wiggles in the inner contour.  
820 Increasing the smoothness by going to  $p = 3$ ,  $r = 2$  shows that the Approx.  $C^1$  method predicts  
821 the stress field very well over the whole domain but with the wiggles in the inner contour, and  
822 that the D-patch suffers from the singularity at the EVs. Lastly, the  $p = 4$ ,  $r = 2$  plots show that  
823 the wiggles in the inner contour are eliminated for the Approx.  $C^1$  and the AS- $G^1$  methods and  
824 that the artifacts of the D-patch around the EV are still there but to a lesser extent. Finally, the  
825 results of the penalty method in Fig. 16 show it is able to provide an accurate representation of  
826 the stress fields. As seen from Fig. 13, penalty factors  $\alpha = 1$  and  $\alpha = 10$  provide good conver-  
827 gence in the bending energy norm. Indeed, the stress fields for the fixed  $64 \times 64$  element meshes  
828 in Fig. 16 confirm that for these penalty factors the stress fields accurately represent the single  
829 patch stress fields, despite small artifacts around the EVs for  $\alpha = 1$ . For a higher penalty factor  
830 of  $\alpha = 100$ , the stress fields following from the penalty method are not guaranteed to be accurate,  
831 showing the downside of this method.

832  
833 Overall, the stress analysis for multiple combinations and regularities shows that the Almost-  
834  $C^1$  method is generally unfavourable since it is only applicable for  $p = 2$ ,  $r = 1$  hence  $C^0$  stress  
835 fields, suffering from a lack of continuity over the whole domain. This also makes the D-patch as  
836 applicable as the Approx.  $C^1$  method in terms of degree and regularity combinations. Comparing  
837 the D-patch with the Approx.  $C^1$  and the AS- $G^1$  methods, it is shown that the D-patch suffers  
838 from the singularity in the EVs when reconstructing stresses, whereas the other two methods are  
839 able to recover the stress fields without problems. Moreover, this example has also shown the  
840 advantage of smooth unstructured spline constructions for stress analyses, since their continuity  
841 across (almost) all of the domain is ensured, contrary to the penalty method. Lastly, this example  
842 shows the advantage of IGA in general over lower-order methods like FEA, since the higher-  
843 degree bases (e.g.  $p = 4$ ,  $r = 2$ ) provides smooth stress fields compared to lower-degree bases  
844 ( $p = 2$ ,  $r = 1$ ).

#### 846 4.6. Conclusions

847 In this section a quantitative comparison of the AS- $G^1$ , the Approx.  $C^1$ , the D-Patch and the  
848 Almost- $C^1$  constructions is provided. The methods have been assessed on different aspects: i)  
849 convergence of the biharmonic equation (Section 4.1); ii) convergence of the linear Kirchhoff-  
850 Love shell (Section 4.2); iii) eigenvalue spectrum approximation (Section 4.3); iv) application  
851 to a large-scale complex geometry (Section 4.4) and; v) the reconstruction of stress fields (Sec-  
852 tion 4.5). From these analyses, the following conclusions can be drawn:

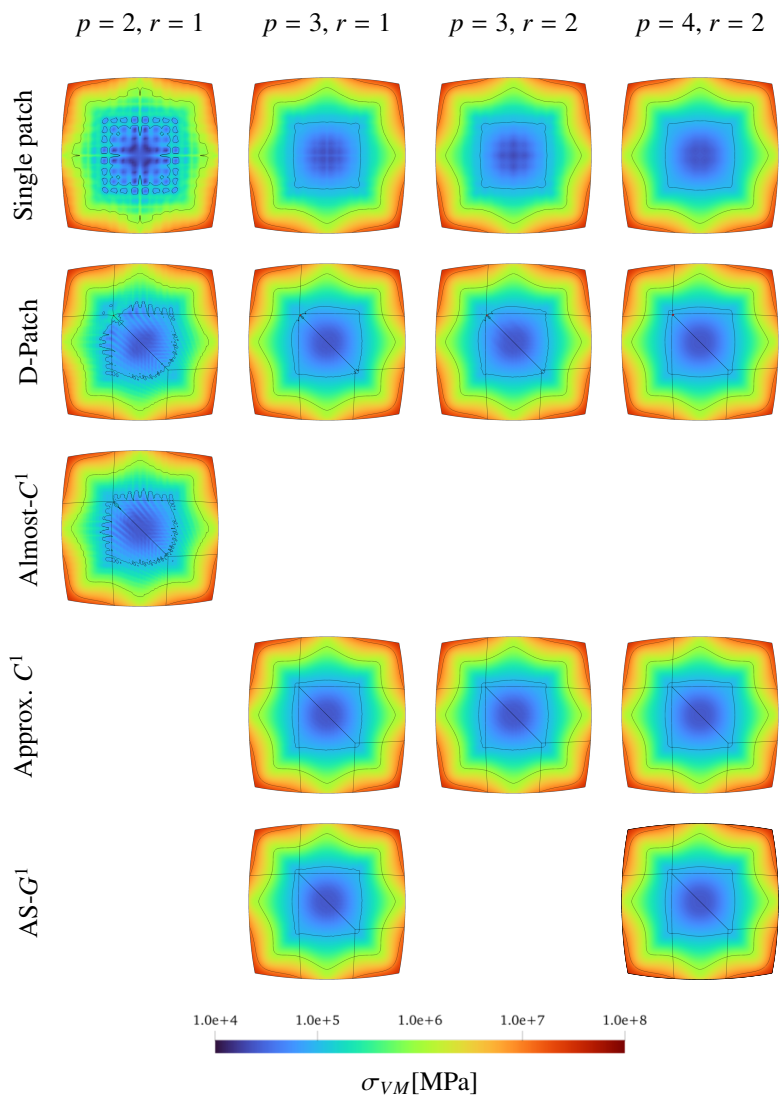


Figure 16: (Caption on next page).

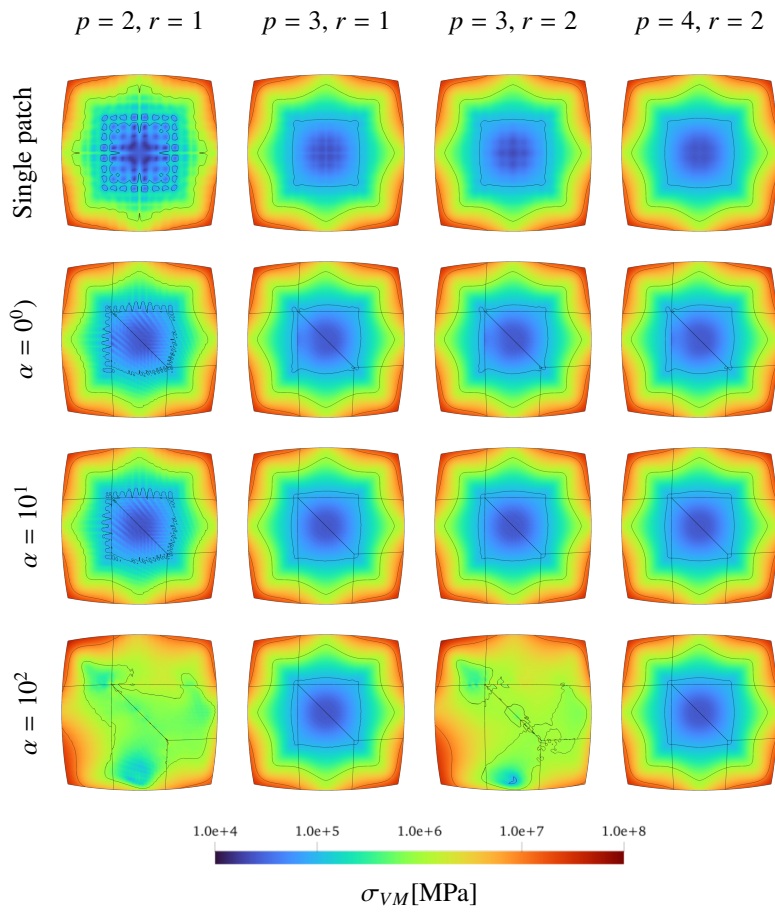


Figure 16: Von Mises membrane stress fields for the single patch, unstructured splines and penalty-coupled multi-patch paraboloid from Section 4.2 and Fig. 13 with  $64 \times 64$  elements per patch. The results are provided for different combinations of degree  $p$  and regularity  $r$ . The color bar represents the stress and the contours are plotted for stress levels  $\sigma_{VM} \in \{10^5, 10^6, 10^7\}$  [MPa].



- 853 • All methods converge in a theoretical setting to the same solution for the biharmonic equa-  
854 tion (Sections 4.1 and 4.2). However, the convergence behaviour of the D-Patch method  
855 is sub-optimal and affected by conditioning issues for large meshes. Furthermore, the Ap-  
856 prox.  $C^1$  and AS- $G^1$  methods give worse convergence compared to other methods for the  
857 hyperbolic paraboloid shell but good convergence rates for the elliptic paraboloid shell  
858 example.
  - 859 • From a spectral analysis on the biharmonic equation Section 4.3 it can be concluded that  
860 there is no best unstructured spline construction. Depending on the degree and regularity,  
861 small difference in the eigenvalue spectra are observed between the methods. Comparing  
862 with Nitsche’s method, however, it is concluded that the unstructured spline constructions  
863 considered in this paper perform consistently better. This is also confirmed by the applied  
864 modal analysis on the car geometry Section 4.4, where penalty method fails to find accurate  
865 eigenfrequencies, possibly because of an unsuitable penalty parameter.
  - 866 • From the applied modal analysis on a complex geometry, it can also be concluded that  
867 the Almost- $C^1$  and D-Patch constructions are more straight-forward to apply to a complex  
868 geometry extracted from a mesh. This is due to the fact that the Approx.  $C^1$  and AS-  
869  $G^1$  constructions require, respectively, a  $G^2$  geometry and an analysis-suitable geometry,  
870 which are both not trivial to construct from an originally  $C^0$ -continuous mesh. Instead, the  
871 D-Patch and Almost- $C^1$  constructions require a  $C^1$  geometry, which is easier to construct  
872 in general.
  - 873 • From the stress fields presented in Section 4.5 following from the analysis in Section 4.2, it  
874 can be concluded that the AS- $G^1$  and Approx.  $C^1$  methods provide excellent stress fields.  
875 The D-Patch also provides good stress fields, but inaccuracies are found around the EVs,  
876 possibly because of the singularity close to the EV. The Almost- $C^1$  method is considered  
877 inaccurate for stress analysis because of a lack of higher-degree generalizations. Lastly,  
878 comparison with penalty methods shows that the unstructured spline constructions gener-  
879 ally provide a robust parameter-free approach for coupling, whereas the penalty method  
880 requires careful selection of the penalty parameter.
- 881 Overall, our finding suggest that the Almost- $C^1$  and D-Patch are generally easier to construct,  
882 but for certain problems they have limited accuracy. On the other hand, the AS- $G^1$  or Approx.  $C^1$   
883 discretisations require more pre-processing efforts, but provide optimal convergence, hence ac-  
884 curacy. This, however, depends on the input geometry: generic quad-meshes might require more  
885 pre-processing efforts than  $C^1$ -matching parameterisations. Lastly, the results provided in this  
886 section have shown that strong coupling methods have certain advantages over weak methods,  
887 and therefore provide an interesting alternative.

## 888 5. Conclusions and future work

889 In this paper, we provide a qualitative and quantitative comparison of unstructured spline  
890 constructions for smooth multi-patches in isogeometric analysis. The general advantage of un-  
891 structured spline constructions over trimming or variational coupling methods is that they are  
892 parameter-free, do not require specialized solvers and are typically once constructed in a shape  
893 optimization workflow. The goal of this paper is to compare the analysis-suitable  $G^1$  (AS- $G^1$ )



894 the approximate  $C^1$  (Approx.  $C^1$ ), the degenerate patches (D-Patch) and the Almost- $C^1$  construc-  
895 tions with respect to qualitative aspects (i.e. constraints for application) and quantitative aspects  
896 (i.e. numerical performance).

897

898 From the qualitative analysis, it followed that each method required a different set of con-  
899 straints to be satisfied before the constructions could be applied, see Fig. 7 and Table 1. Degree  
900 and regularity constraints can be satisfied by knot insertion routines or re-fitting, which are rel-  
901 atively straight-forward. The constraint on analysis-suitability for the AS- $G^1$  and the constraint  
902 on  $G^2$  continuity for the Approx.  $C^1$  method require dedicated reparametrisation routines, such  
903 as the one presented by [85]. The fact that D-Patches are restricted to geometries without bound-  
904 ary extraordinary vertices requires redefinition of the quadrilateral mesh. Lastly, the fact that  
905 the Almost- $C^1$  method is only defined for bi-quadratic bases ( $p = 2$ ) restricts the inter-element  
906 continuity to  $C^1$  through the whole domain. Depending on the application and the availability of  
907 existing routines in software, different unstructured spline constructions are favourable, depend-  
908 ing on the geometric flexibility or desired degree and regularity .

909

910 From the quantitative analysis, some conclusions can be drawn on the considered unstruc-  
911 tured spline constructions and between unstructured spline constructions compared to variational  
912 methods such as Nitsche’s method or a penalty method. From the analysis, it was in general ob-  
913 served that depending on the problem type, the different methods have their advantages and  
914 disadvantages. Firstly, simple biharmonic equations (see Section 4.1) and linear shells (see Sec-  
915 tion 4.2) provided good results for all methods. However, the AS- $G^1$  and Approx.  $C^1$  meth-  
916 ods showed slow convergence for the double-curved shell and the D-patch suffered from ill-  
917 conditioning for fine meshes. The Almost- $C^1$  provided good results in general, however it is  
918 only applicable on bi-quadratic splines. Secondly, all methods showed superiority over Nitsche’s  
919 method for the computation of an eigenvalue spectrum for plate vibrations (see Section 4.3)  
920 and no significant differences between the unstructured spline constructions have been observed.  
921 Thirdly, the D-Patch and Almost- $C^1$  showed straight-forward applicability on the problem of a  
922 complex geometry (see Section 4.4), whereas the analysis-suitability requirement of the AS- $G^1$   
923 method and the smoothness requirement of the Approx.  $C^1$  method are non-trivial to satisfy on  
924 off-the-shelf industrial geometries.

925

926 For the penalty method, no suitable penalty parameter was found, and probably optimal  
927 penalty parameters should be chosen per interface rather than globally. Lastly, the AS- $G^1$  and  
928 Approx.  $C^1$  methods provided superior results for stress reconstruction, where the D-Patch suf-  
929 fered around the EVs due to its singular parameterization and the Almost- $C^1$  method provided  
930 bad results due to a lack of higher degrees.

931

932 In conclusion, both comparisons provide an overview of the applicability of the methods  
933 with respect to the requirements needed to construct them, on the notions of nestedness and in  
934 general on the performance of the methods. Overall, it can be concluded from both analyses  
935 that among the compared methods, there is no general best construction. More precisely, the  
936 quantitative analysis shows that different methods perform differently in different applications,  
937 given that they can be constructed. Furthermore, with the backgrounds and properties provided  
938 in the qualitative analysis section, we hope that the present paper provides valuable insights for  
939 application of the considered methods to multi-patch problems.

940

941 In addition, the comparisons in the present paper provide directions for the improvements of  
942 the considered methods. For the AS- $G^1$  and Approx.  $C^1$  methods, restrictions on geometry and  
943 parameterization are a bottleneck in the industrial applications. Therefore, it is recommended  
944 to expand the applicability of these methods by developing dedicated geometric pre-processing  
945 routines. For the D-Patch construction, the limitation of the construction of the basis near  $\nu > 3$   
946 boundary EVs calls for the development of routines to eliminate these EVs in quadrilateral multi-  
947 patches, as discussed in the qualitative comparison. Furthermore, the example of the bi-harmonic  
948 equation has shown that the D-Patch can suffer from ill-conditioned system, hence development  
949 of pre-conditioners for D-Patch constructions is advised. Lastly, although the Almost- $C^1$  resolves  
950 the downsides of the D-Patch construction, its restriction on the degree of the spline-space is a  
951 major disadvantage when plotting stress fields in shell analysis. Therefore, for the Almost- $C^1$   
952 construction it is recommended to explore expansion to higher degrees.

### 953 Acknowledgements

954 HMV is grateful to Delft University of Technology, specifically the faculty of Electrical Engi-  
955 neering, Mathematics and Computer Science (EEMCS) and the faculty of Mechanical, Maritime  
956 and Materials Engineering (3mE) for the financial support to conduct this research. AM ac-  
957 knowledges support from EU's Horizon 2020 research under the Marie Skłodowska-Curie grant  
958 860843 and DT is grateful to ANSYS Inc. for their financial support. Furthermore, the authors  
959 thank Wei Jun Wong from Delft University of Technology for delivering the ABAQUS refer-  
960 ence results, and the community of the Geometry + Simulation Modules (a.k.a. gismo) for their  
961 continuous effort on improving the code.

### 962 References

- 963 [1] T. Hughes, J. A. Cottrell, Y. Bazilevs, Isogeometric analysis: CAD, finite elements, NURBS, exact geometry  
964 and mesh refinement, *Computer Methods in Applied Mechanics and Engineering* 194 (39-41) (2005) 4135–4195.  
965 [arXiv:1608.04366](https://arxiv.org/abs/1608.04366), [doi:10.1016/j.cma.2004.10.008](https://doi.org/10.1016/j.cma.2004.10.008).
- 966 [2] A. Bressan, E. Sande, *Approximation in FEM, DG and IGA: a theoretical comparison*, *Numer. Math.* 143 (4)  
967 (2019) 923–942. [arXiv:1808.04163](https://arxiv.org/abs/1808.04163), [doi:10.1007/s00211-019-01063-5](https://doi.org/10.1007/s00211-019-01063-5).  
968 URL <https://doi.org/10.1007/s00211-019-01063-5>
- 969 [3] E. Sande, C. Manni, H. Speleers, *Explicit error estimates for spline approximation of arbitrary smooth-*  
970 *ness in isogeometric analysis*, *Numer. Math.* 144 (4) (2020) 889–929. [arXiv:1909.03559](https://arxiv.org/abs/1909.03559), [doi:10.1007/s00211-019-01097-9](https://doi.org/10.1007/s00211-019-01097-9).  
971 URL <https://doi.org/10.1007/s00211-019-01097-9>
- 972 [4] J. Cottrell, A. Reali, Y. Bazilevs, T. Hughes, Isogeometric analysis of structural vibrations, *Computer Methods in*  
973 *Applied Mechanics and Engineering* 195 (41-43) (2006) 5257–5296. [doi:10.1016/J.CMA.2005.09.027](https://doi.org/10.1016/J.CMA.2005.09.027).
- 974 [5] T. J. R. Hughes, A. Reali, G. Sangalli, Duality and unified analysis of discrete approximations in structural dynam-  
975 ics and wave propagation: Comparison of p-method finite elements with k-method NURBS, *Computer Methods*  
976 *in Applied Mechanics and Engineering* 197 (49) (2008) 4104–4124. [doi:10.1016/j.cma.2008.04.006](https://doi.org/10.1016/j.cma.2008.04.006).
- 977 [6] T. J. R. Hughes, J. A. Evans, A. Reali, Finite element and NURBS approximations of eigenvalue, boundary-  
978 value, and initial-value problems, *Computer Methods in Applied Mechanics and Engineering* 272 (2014) 290–  
979 320. [doi:10.1016/j.cma.2013.11.012](https://doi.org/10.1016/j.cma.2013.11.012).
- 980 [7] F. Xu, S. Morganti, R. Zakerzadeh, D. Kamensky, F. Auricchio, A. Reali, T. J. R. Hughes, M. S. Sacks, M.-C. Hsu,  
981 *A framework for designing patient-specific bioprosthetic heart valves using immersogeometric fluid-structure*  
982 *interaction analysis*, *Int. j. numer. method. biomed. eng.* 34 (4) (2018) e2938. [doi:10.1002/cnm.2938](https://doi.org/10.1002/cnm.2938).  
983 URL <http://doi.wiley.com/10.1002/cnm.2938>
- 984 [8] A. Farahat, B. Jüttler, M. Kapl, T. Takacs, Isogeometric analysis with  $C^1$ -smooth functions over multi-patch  
985 surfaces, *Computer Methods in Applied Mechanics and Engineering* 403 (2023) 115706. [doi:10.1016/j.cma.2022.115706](https://doi.org/10.1016/j.cma.2022.115706).  
986  
987

- 988 [9] P. Weinmüller, T. Takacs, Construction of approximate C1 bases for isogeometric analysis on two-patch domains,  
 989 Computer Methods in Applied Mechanics and Engineering 385 (2021) 114017. [arXiv:2103.02980](https://arxiv.org/abs/2103.02980), [doi:10.1016/j.cma.2021.114017](https://doi.org/10.1016/j.cma.2021.114017).
- 990 [10] D. Toshniwal, H. Speleers, T. J. Hughes, Smooth cubic spline spaces on unstructured quadrilateral meshes with  
 991 particular emphasis on extraordinary points: Geometric design and isogeometric analysis considerations, Com-  
 992 puter Methods in Applied Mechanics and Engineering 327 (2017) 411–458. [doi:10.1016/j.cma.2017.06.](https://doi.org/10.1016/j.cma.2017.06.008)  
 993 [008](https://doi.org/10.1016/j.cma.2017.06.008).
- 994 [11] T. Takacs, D. Toshniwal, Almost-C1 splines: Biquadratic splines on unstructured quadrilateral meshes and their  
 995 application to fourth order problems, Computer Methods in Applied Mechanics and Engineering 403 (2023)  
 996 115640. [doi:10.1016/j.cma.2022.115640](https://doi.org/10.1016/j.cma.2022.115640).
- 997 [12] J. Kiendl, K.-U. Bletzinger, J. Linhard, R. Wüchner, Isogeometric shell analysis with Kirchhoff–Love elements,  
 998 Computer Methods in Applied Mechanics and Engineering 198 (49–52) (2009) 3902–3914. [doi:10.1016/J.](https://doi.org/10.1016/J.CMA.2009.08.013)  
 999 [CMA.2009.08.013](https://doi.org/10.1016/J.CMA.2009.08.013).
- 1000 [13] H. Gómez, V. M. Calo, Y. Bazilevs, T. J. R. Hughes, Isogeometric analysis of the Cahn–Hilliard phase-field model,  
 1001 Computer Methods in Applied Mechanics and Engineering 197 (49) (2008) 4333–4352. [doi:10.1016/j.cma.](https://doi.org/10.1016/j.cma.2008.05.003)  
 1002 [2008.05.003](https://doi.org/10.1016/j.cma.2008.05.003).
- 1003 [14] F. Massarwi, B. van Sossin, G. Elber, Untrimming: Precise conversion of trimmed-surfaces to tensor-product  
 1004 surfaces, Computers & Graphics 70 (2018) 80–91. [doi:10.1016/j.cag.2017.08.009](https://doi.org/10.1016/j.cag.2017.08.009).
- 1005 [15] R. R. Hiemstra, K. M. Shepherd, M. J. Johnson, L. Quan, T. J. R. Hughes, Towards untrimmed NURBS:  
 1006 CAD embedded reparameterization of trimmed B-rep geometry using frame-field guided global parameteriza-  
 1007 tion, Computer Methods in Applied Mechanics and Engineering 369 (2020) 113227. [doi:10.1016/j.cma.](https://doi.org/10.1016/j.cma.2020.113227)  
 1008 [2020.113227](https://doi.org/10.1016/j.cma.2020.113227).
- 1009 [16] K. Rafetseder, W. Zulehner, A decomposition result for kirchhoff plate bending problems and a new discretization  
 1010 approach, SIAM Journal on Numerical Analysis 56 (3) (2018) 1961–1986.
- 1011 [17] K. Rafetseder, W. Zulehner, A new mixed approach to Kirchhoff–Love shells, Computer Methods in Applied  
 1012 Mechanics and Engineering 346 (2019) 440–455. [doi:10.1016/j.cma.2018.11.033](https://doi.org/10.1016/j.cma.2018.11.033).
- 1013 [18] V. Kosin, S. Beuchler, T. Wick, A new mixed method for the biharmonic eigenvalue problem, Computers &  
 1014 Mathematics with Applications 136 (2023) 44–53.
- 1015 [19] B. Marussig, T. J. R. Hughes, A Review of Trimming in Isogeometric Analysis: Challenges, Data Exchange  
 1016 and Simulation Aspects, Archives of Computational Methods in Engineering 25 (4) (2018) 1059–1127. [doi:](https://doi.org/10.1007/s11831-017-9220-9)  
 1017 [10.1007/s11831-017-9220-9](https://doi.org/10.1007/s11831-017-9220-9).
- 1018 [20] J. Parvizian, A. Düster, E. Rank, Finite cell method, Computational Mechanics 41 (1) (2007) 121–133. [doi:](https://doi.org/10.1007/s00466-007-0173-y)  
 1019 [10.1007/s00466-007-0173-y](https://doi.org/10.1007/s00466-007-0173-y).
- 1020 [21] A. Düster, J. Parvizian, Z. Yang, E. Rank, The finite cell method for three-dimensional problems of solid  
 1021 mechanics, Computer Methods in Applied Mechanics and Engineering 197 (45) (2008) 3768–3782. [doi:](https://doi.org/10.1016/j.cma.2008.02.036)  
 1022 [10.1016/j.cma.2008.02.036](https://doi.org/10.1016/j.cma.2008.02.036).
- 1023 [22] D. Schillinger, M. Ruess, The Finite Cell Method: A Review in the Context of Higher-Order Structural Analysis  
 1024 of CAD and Image-Based Geometric Models, Archives of Computational Methods in Engineering 22 (3) (2015)  
 1025 391–455. [doi:10.1007/s11831-014-9115-y](https://doi.org/10.1007/s11831-014-9115-y).
- 1026 [23] E. Burman, S. Claus, P. Hansbo, M. G. Larson, A. Massing, CutFEM: Discretizing geometry and partial  
 1027 differential equations, International Journal for Numerical Methods in Engineering 104 (7) (2015) 472–501.  
 1028 [doi:10.1002/nme.4823](https://doi.org/10.1002/nme.4823).
- 1029 [24] M.-C. Hsu, C. Wang, F. Xu, A. J. Herrema, A. Krishnamurthy, Direct immersogeometric fluid flow analysis using  
 1030 B-rep CAD models, Computer Aided Geometric Design 43 (2016) 143–158. [doi:10.1016/J.CAGD.2016.02.](https://doi.org/10.1016/J.CAGD.2016.02.007)  
 1031 [007](https://doi.org/10.1016/J.CAGD.2016.02.007).
- 1032 [25] D. Kamensky, M.-C. Hsu, D. Schillinger, J. A. Evans, A. Aggarwal, Y. Bazilevs, M. S. Sacks, An immerso-  
 1033 geo-  
 1034 metric variational framework for fluid–structure interaction: Application to bioprosthetic heart valves, Computer  
 1035 Methods in Applied Mechanics and Engineering 284 (2015) 1005–1053. [doi:10.1016/J.CMA.2014.10.040](https://doi.org/10.1016/J.CMA.2014.10.040).
- 1036 [26] F. de Prenter, C. Verhoosel, H. van Brummelen, M. Larson, S. Badia, Stability and conditioning of immersed  
 1037 finite element methods: Analysis and remedies (Aug. 2022). [arXiv:arXiv:2208.08538](https://arxiv.org/abs/2208.08538).
- 1038 [27] S. C. Divi, C. V. Verhoosel, F. Auricchio, A. Reali, E. H. van Brummelen, Error-estimate-based adaptive integra-  
 1039 tion for immersed isogeometric analysis, Computers & Mathematics with Applications 80 (11) (2020) 2481–2516.  
 1040 [doi:10.1016/j.camwa.2020.03.026](https://doi.org/10.1016/j.camwa.2020.03.026).
- 1041 [28] F. de Prenter, C. V. Verhoosel, E. H. van Brummelen, J. A. Evans, C. Messe, J. Benzaken, K. Maute, Multigrid  
 1042 solvers for immersed finite element methods and immersed isogeometric analysis, Computational Mechanics  
 1043 65 (3) (2020) 807–838. [doi:10.1007/s00466-019-01796-y](https://doi.org/10.1007/s00466-019-01796-y).
- 1044 [29] Y. Guo, M. Ruess, Weak Dirichlet boundary conditions for trimmed thin isogeometric shells, Computers & Math-  
 1045 ematics with Applications 70 (7) (2015) 1425–1440. [doi:10.1016/J.CAMWA.2015.06.012](https://doi.org/10.1016/J.CAMWA.2015.06.012).
- 1046 [30] Y. Guo, J. Heller, T. J. Hughes, M. Ruess, D. Schillinger, Variationally consistent isogeometric analysis of trimmed

- thin shells at finite deformations, based on the STEP exchange format. *Computer Methods in Applied Mechanics and Engineering* 336 (2018) 39–79. doi:10.1016/j.cma.2018.02.027.
- [31] L. Coradello, D. D’Angella, M. Carraturo, J. Kiendl, S. Kollmannsberger, E. Rank, A. Reali, Hierarchically refined isogeometric analysis of trimmed shells, *Computational Mechanics* 66 (2) (2020) 431–447. doi:10.1007/s00466-020-01858-6.
- [32] L. Coradello, P. Antolin, R. Vázquez, A. Buffa, Adaptive isogeometric analysis on two-dimensional trimmed domains based on a hierarchical approach, *Computer Methods in Applied Mechanics and Engineering* 364 (2020) 112925. doi:10.1016/j.cma.2020.112925.
- [33] L. Coradello, J. Kiendl, A. Buffa, Coupling of non-conforming trimmed isogeometric Kirchhoff–Love shells via a projected super-penalty approach, *Computer Methods in Applied Mechanics and Engineering* 387 (2021) 114187. arXiv:2104.13804, doi:10.1016/J.CMA.2021.114187.
- [34] Y. Guo, M. Ruess, D. Schillinger, A parameter-free variational coupling approach for trimmed isogeometric thin shells, *Computational Mechanics* 59 (4) (2017) 693–715. doi:10.1007/S00466-016-1368-X/FIGURES/33.
- [35] L. F. Leidingner, M. Breitenberger, A. M. Bauer, S. Hartmann, R. Wüchner, K. U. Bletzinger, F. Duddeck, L. Song, Explicit dynamic isogeometric B-Rep analysis of penalty-coupled trimmed NURBS shells, *Computer Methods in Applied Mechanics and Engineering* 351 (2019) 891–927. doi:10.1016/j.cma.2019.04.016.
- [36] K. Paul, C. Zimmermann, T. X. Duong, R. A. Sauer, Isogeometric continuity constraints for multi-patch shells governed by fourth-order deformation and phase field models, *Computer Methods in Applied Mechanics and Engineering* 370. arXiv:2001.05964, doi:10.1016/j.cma.2020.113219.
- [37] J. Kiendl, Isogeometric analysis and shape optimal design of shell structures, Ph.D. thesis, Technische Universität München (2011).
- [38] J. Kiendl, Y. Bazilevs, M.-C. Hsu, R. Wüchner, K.-U. Bletzinger, The bending strip method for isogeometric analysis of Kirchhoff–Love shell structures comprised of multiple patches, *Computer Methods in Applied Mechanics and Engineering* 199 (37-40) (2010) 2403–2416. doi:10.1016/J.CMA.2010.03.029.
- [39] J. Nitsche, Über ein Variationsprinzip zur Lösung von Dirichlet-Problemen bei Verwendung von Teilräumen, die keinen Randbedingungen unterworfen sind, *Abhandlungen aus dem Mathematischen Seminar der Universität Hamburg* 36 (1) (1971) 9–15. doi:10.1007/BF02995904.
- [40] M. Ruess, D. Schillinger, Y. Bazilevs, V. Varduhn, E. Rank, Weakly enforced essential boundary conditions for NURBS-embedded and trimmed NURBS geometries on the basis of the finite cell method, *International Journal for Numerical Methods in Engineering* 95 (10) (2013) 811–846. doi:10.1002/nme.4522.
- [41] M. Ruess, D. Schillinger, A. I. Özcan, E. Rank, Weak coupling for isogeometric analysis of non-matching and trimmed multi-patch geometries, *Computer Methods in Applied Mechanics and Engineering* 269 (2014) 46–71. doi:10.1016/J.CMA.2013.10.009.
- [42] D. Schillinger, I. Harari, M.-C. Hsu, D. Kamensky, S. K. F. Stoter, Y. Yu, Y. Zhao, The non-symmetric Nitsche method for the parameter-free imposition of weak boundary and coupling conditions in immersed finite elements, *Computer Methods in Applied Mechanics and Engineering* 309 (2016) 625–652. doi:10.1016/j.cma.2016.06.026.
- [43] Q. Hu, F. Chouly, P. Hu, G. Cheng, S. P. Bordas, Skew-symmetric Nitsche’s formulation in isogeometric analysis: Dirichlet and symmetry conditions, patch coupling and frictionless contact, *Computer Methods in Applied Mechanics and Engineering* 341 (2018) 188–220. arXiv:1711.10253, doi:10.1016/J.CMA.2018.05.024.
- [44] Y. Guo, M. Ruess, Nitsche’s method for a coupling of isogeometric thin shells and blended shell structures, *Computer Methods in Applied Mechanics and Engineering* 284 (2015) 881–905. doi:10.1016/J.CMA.2014.11.014.
- [45] J. Benzaken, J. A. Evans, S. F. McCormick, R. Tamstorf, Nitsche’s method for linear Kirchhoff–Love shells: Formulation, error analysis, and verification, *Computer Methods in Applied Mechanics and Engineering* 374. doi:10.1016/J.CMA.2020.113544.
- [46] X. Du, G. Zhao, W. Wang, H. Fang, Nitsche’s method for non-conforming multipatch coupling in hyperelastic isogeometric analysis, *Computational Mechanics* 65 (3) (2020) 687–710. doi:10.1007/s00466-019-01789-x.
- [47] P. Weinmüller, T. Takacs, An approximate C1 multi-patch space for isogeometric analysis with a comparison to Nitsche’s method, *Computer Methods in Applied Mechanics and Engineering* 401 (2022) 115592. doi:10.1016/j.cma.2022.115592.
- [48] R. Bouclier, J. C. Passieux, A Nitsche-based non-intrusive coupling strategy for global/local isogeometric structural analysis, *Computer Methods in Applied Mechanics and Engineering* 340 (2018) 253–277. doi:10.1016/j.cma.2018.05.022.
- [49] T. X. Duong, F. Roohbakhshan, R. A. Sauer, A new rotation-free isogeometric thin shell formulation and a corresponding continuity constraint for patch boundaries, *Computer Methods in Applied Mechanics and Engineering* 316 (2017) 43–83. doi:10.1016/j.cma.2016.04.008.
- [50] M. Breitenberger, A. Apostolatos, B. Philipp, R. Wüchner, K. U. Bletzinger, Analysis in computer aided design: Nonlinear isogeometric B-Rep analysis of shell structures, *Computer Methods in Applied Mechanics and*

- Engineering 284 (2015) 401–457. doi:10.1016/j.cma.2014.09.033.
- [51] A. J. Herrema, J. Kiendl, M. C. Hsu, A framework for isogeometric-analysis-based optimization of wind turbine blade structures, *Wind Energy* 22 (2) (2019) 153–170. doi:10.1002/we.2276.
- [52] L. Leonetti, F. S. Liguori, D. Magisano, J. Kiendl, A. Reali, G. Garcea, A robust penalty coupling of non-matching isogeometric Kirchhoff–Love shell patches in large deformations, *Computer Methods in Applied Mechanics and Engineering* 371 (2020) 113289. doi:10.1016/j.cma.2020.113289.
- [53] T. Pasch, L. F. Leidinger, A. Apostolatos, R. Wüchner, K. U. Bletzinger, F. Duddeck, A priori penalty factor determination for (trimmed) NURBS-based shells with Dirichlet and coupling constraints in isogeometric analysis, *Computer Methods in Applied Mechanics and Engineering* 377 (2021) 113688. doi:10.1016/j.cma.2021.113688.
- [54] L. Coradello, G. Loli, A. Buffa, A projected super-penalty method for the  $C^1$ -coupling of multi-patch isogeometric Kirchhoff plates, *Computational Mechanics* 67 (4) (2021) 1133–1153. doi:10.1007/s00466-021-01983-w.
- [55] C. Bernardi, Y. Maday, A. T. Patera, Domain Decomposition by the Mortar Element Method, in: H. G. Kaper, M. Garbey, G. W. Pieper (Eds.), *Asymptotic and Numerical Methods for Partial Differential Equations with Critical Parameters*, NATO ASI Series, Springer Netherlands, Dordrecht, 1993, pp. 269–286. doi:10.1007/978-94-011-1810-1\_17.
- [56] C. Hesch, P. Betsch, Isogeometric analysis and domain decomposition methods, *Computer Methods in Applied Mechanics and Engineering* 213–216 (2012) 104–112. doi:10.1016/j.cma.2011.12.003.
- [57] W. Dornisch, G. Vitucci, S. Klinkel, The weak substitution method - an application of the mortar method for patch coupling in NURBS-based isogeometric analysis, *International Journal for Numerical Methods in Engineering* 103 (3) (2015) 205–234. doi:10.1002/nme.4918.
- [58] R. Bouclier, J. C. Passieux, M. Salaün, Development of a new, more regular, mortar method for the coupling of NURBS subdomains within a NURBS patch: Application to a non-intrusive local enrichment of NURBS patches, *Computer Methods in Applied Mechanics and Engineering* 316 (2017) 123–150. doi:10.1016/j.cma.2016.05.037.
- [59] M. Dittmann, S. Schuß, B. Wohlmuth, C. Hesch, Weak  $C_n$  coupling for multipatch isogeometric analysis in solid mechanics, *International Journal for Numerical Methods in Engineering* 118 (11) (2019) 678–699. doi:10.1002/nme.6032.
- [60] M. Dittmann, S. Schuß, B. Wohlmuth, C. Hesch, Crosspoint modification for multi-patch isogeometric analysis, *Computer Methods in Applied Mechanics and Engineering* 360 (2020) 112768. doi:10.1016/j.cma.2019.112768.
- [61] S. Schuß, M. Dittmann, B. Wohlmuth, S. Klinkel, C. Hesch, Multi-patch isogeometric analysis for Kirchhoff–Love shell elements, *Computer Methods in Applied Mechanics and Engineering* 349 (2019) 91–116. doi:10.1016/J.CMA.2019.02.015.
- [62] A. Benvenuti, G. Loli, G. Sangalli, T. Takacs, Isogeometric multi-patch  $C^1$ -mortar coupling for the biharmonic equation (Mar. 2023). arXiv:2303.07255, doi:10.48550/arXiv.2303.07255.
- [63] E. Brivadis, A. Buffa, B. Wohlmuth, L. Wunderlich, Isogeometric mortar methods, *Computer Methods in Applied Mechanics and Engineering* 284 (2015) 292–319. doi:10.1016/j.cma.2014.09.012.
- [64] B. I. Wohlmuth, A Mortar Finite Element Method Using Dual Spaces for the Lagrange Multiplier, *SIAM Journal on Numerical Analysis* 38 (3) (2000) 989–1012. doi:10.1137/S0036142999350929.
- [65] Z. Zou, M. A. Scott, M. J. Borden, D. C. Thomas, W. Dornisch, E. Brivadis, Isogeometric Bézier dual mortaring: Refineable higher-order spline dual bases and weakly continuous geometry, *Computer Methods in Applied Mechanics and Engineering* 333 (2018) 497–534. doi:10.1016/j.cma.2018.01.023.
- [66] D. Miao, Z. Zou, M. A. Scott, M. J. Borden, D. C. Thomas, Isogeometric Bézier dual mortaring: The Kirchhoff–Love shell problem, *Computer Methods in Applied Mechanics and Engineering* 382 (2021) 113873. doi:10.1016/j.cma.2021.113873.
- [67] L. Wunderlich, A. Seitz, M. D. Alaydin, B. Wohlmuth, A. Popp, Biorthogonal splines for optimal weak patch-coupling in isogeometric analysis with applications to finite deformation elasticity, *Computer Methods in Applied Mechanics and Engineering* 346 (2019) 197–215. doi:10.1016/j.cma.2018.11.024.
- [68] T. Horger, A. Reali, B. Wohlmuth, L. Wunderlich, A hybrid isogeometric approach on multi-patches with applications to Kirchhoff plates and eigenvalue problems, *Computer Methods in Applied Mechanics and Engineering* 348 (2019) 396–408. doi:10.1016/j.cma.2018.12.038.
- [69] A. Apostolatos, K.-U. Bletzinger, R. Wüchner, Weak imposition of constraints for structural membranes in transient geometrically nonlinear isogeometric analysis on multipatch surfaces, *Computer Methods in Applied Mechanics and Engineering* 350 (2019) 938–994. doi:10.1016/J.CMA.2019.01.023.
- [70] C. Hesch, U. Khristenko, R. Krause, A. Popp, A. Seitz, W. Wall, B. Wohlmuth, *Frontiers in Mortar Methods for Isogeometric Analysis*, in: J. Schröder, P. Wriggers (Eds.), *Non-Standard Discretisation Methods in Solid Mechanics*, Lecture Notes in Applied and Computational Mechanics, Springer International Publishing, Cham, 2022, pp. 405–447. doi:10.1007/978-3-030-92672-4\_15.



- 1165 [71] W. Dornisch, J. Stöckler, An isogeometric mortar method for the coupling of multiple NURBS do-  
 1166 mains with optimal convergence rates, *Numerische Mathematik* 149 (4) (2021) 871–931. doi:10.1007/  
 1167 s00211-021-01246-z.
- 1168 [72] F. Cirak, Q. Long, Subdivision shells with exact boundary control and non-manifold geometry, *International*  
 1169 *Journal for Numerical Methods in Engineering* 88 (9) (2011) 897–923. doi:10.1002/nme.3206.
- 1170 [73] L. Ying, D. Zorin, Nonmanifold subdivision, in: *Proceedings Visualization, 2001. VIS '01.*, 2001, pp. 325–569.  
 1171 doi:10.1109/VISUAL.2001.964528.
- 1172 [74] M. Moulaeifard, F. Wellmann, S. Bernard, M. de la Varga, D. Bommers, Subdivide and Conquer: Adapting  
 1173 Non-Manifold Subdivision Surfaces to Surface-Based Representation and Reconstruction of Complex Geolog-  
 1174 ical Structures, *Mathematical Geosciences* 55 (1) (2023) 81–111. doi:10.1007/s11004-022-10017-x.
- 1175 [75] T. J. Hughes, G. Sangalli, T. Takacs, D. Toshniwal, Smooth multi-patch discretizations in Isogeometric Analysis,  
 1176 *Handbook of Numerical Analysis* 22 (2021) 467–543. doi:10.1016/bs.hna.2020.09.002.
- 1177 [76] D. Groisser, J. Peters, Matched Gk-constructions always yield Ck-continuous isogeometric elements, *Computer*  
 1178 *Aided Geometric Design* 34 (2015) 67–72. doi:10.1016/j.cagd.2015.02.002.
- 1179 [77] M. Majeed, F. Cirak, Isogeometric analysis using manifold-based smooth basis functions, *Computer Methods in*  
 1180 *Applied Mechanics and Engineering* 316 (2017) 547–567. doi:10.1016/j.cma.2016.08.013.
- 1181 [78] X. Yuan, W. Ma, Mapped B-spline basis functions for shape design and isogeometric analysis over an arbitrary  
 1182 parameterization, *Computer Methods in Applied Mechanics and Engineering* 269 (2014) 87–107. doi:10.1016/  
 1183 j.cma.2013.10.023.
- 1184 [79] M. Kapl, V. Vitrih, B. Jüttler, K. Birner, Isogeometric analysis with geometrically continuous functions on two-  
 1185 patch geometries, *Computers & Mathematics with Applications* 70 (7) (2015) 1518–1538. doi:10.1016/j.  
 1186 camwa.2015.04.004.
- 1187 [80] M. Kapl, F. Buchegger, M. Bercovier, B. Jüttler, Isogeometric analysis with geometrically continuous functions on  
 1188 planar multi-patch geometries, *Computer Methods in Applied Mechanics and Engineering* 316 (2017) 209–234.  
 1189 doi:10.1016/j.cma.2016.06.002.
- 1190 [81] M. Kapl, G. Sangalli, T. Takacs, A family of  $C^1$  quadrilateral finite elements, *Advances in Computational Mathe-*  
 1191 *matics* 47 (6) (2021) 82. doi:10.1007/s10444-021-09878-3.
- 1192 [82] J. Grošelj, M. Kapl, M. Knez, T. Takacs, V. Vitrih, A super-smooth  $C^1$  spline space over planar mixed triangle and  
 1193 quadrilateral meshes, *Computers & Mathematics with Applications* 80 (12) (2020) 2623–2643. doi:10.1016/  
 1194 j.camwa.2020.10.004.
- 1195 [83] M. Kapl, V. Vitrih, Cs-smooth isogeometric spline spaces over planar bilinear multi-patch parameterizations,  
 1196 *Advances in Computational Mathematics* 47 (3) (2021) 47. doi:10.1007/s10444-021-09868-5.
- 1197 [84] A. Collin, G. Sangalli, T. Takacs, Analysis-suitable  $G^1$  multi-patch parametrizations for  $C^1$  isogeometric spaces,  
 1198 *Computer Aided Geometric Design* 47 (2016) 93–113. doi:10.1016/j.cagd.2016.05.009.
- 1199 [85] M. Kapl, G. Sangalli, T. Takacs, Construction of analysis-suitable  $G^1$  planar multi-patch parameterizations,  
 1200 *Computer-Aided Design* 97 (2018) 41–55. doi:10.1016/j.cad.2017.12.002.
- 1201 [86] A. Farahat, H. M. Verhelst, J. Kiendl, M. Kapl, Isogeometric analysis for multi-patch structured Kirchhoff–Love  
 1202 shells, *Computer Methods in Applied Mechanics and Engineering* 411 (2023) 116060. doi:10.1016/j.cma.  
 1203 2023.116060.
- 1204 [87] M. Reichle, J. Arf, B. Simeon, S. Klinkel, Smooth multi-patch scaled boundary isogeometric analysis for  
 1205 Kirchhoff–Love shells (Apr. 2023). arXiv:2304.05857, doi:10.48550/arXiv.2304.05857.
- 1206 [88] J. Arf, M. Reichle, S. Klinkel, B. Simeon, Scaled boundary isogeometric analysis with  $C^1$  coupling for Kirchhoff  
 1207 plate theory, *Computer Methods in Applied Mechanics and Engineering* 415 (2023) 116198. doi:10.1016/j.  
 1208 cma.2023.116198.
- 1209 [89] U. Reif, A Refineable Space of Smooth Spline Surfaces of Arbitrary Topological Genus, *Journal of Approximation*  
 1210 *Theory* 90 (2) (1997) 174–199. doi:10.1006/jath.1996.3079.
- 1211 [90] T. Nguyen, J. Peters, Refinable  $C^1$  spline elements for irregular quad layout, *Computer Aided Geometric Design*  
 1212 43 (2016) 123–130. doi:10.1016/j.cagd.2016.02.009.
- 1213 [91] H. Casquero, X. Wei, D. Toshniwal, A. Li, T. J. Hughes, J. Kiendl, Y. J. Zhang, Seamless integration of design  
 1214 and Kirchhoff–Love shell analysis using analysis-suitable unstructured T-splines, *Computer Methods in Applied*  
 1215 *Mechanics and Engineering* 360 (2020) 112765. doi:10.1016/j.cma.2019.112765.
- 1216 [92] X. Wei, X. Li, K. Qian, T. J. R. Hughes, Y. J. Zhang, H. Casquero, Analysis-suitable unstructured T-splines:  
 1217 Multiple extraordinary points per face, *Computer Methods in Applied Mechanics and Engineering* 391 (2022)  
 1218 114494. doi:10.1016/j.cma.2021.114494.
- 1219 [93] P. J. Barendrecht, Isogeometric analysis for subdivision surfaces, Eindhoven University of Technology: Eind-  
 1220 hoven, The Netherlands.
- 1221 [94] A. Riffnaller-Schiefer, U. H. Augsdörfer, D. W. Fellner, Isogeometric shell analysis with nurbs compatible subdivi-  
 1222 sion surfaces, *Applied Mathematics and Computation* 272 (2016) 139–147.
- 1223 [95] Q. Pan, G. Xu, G. Xu, Y. Zhang, Isogeometric analysis based on extended catmull–clark subdivision, *Computers*

- 1224 & Mathematics with Applications 71 (1) (2016) 105–119.
- 1225 [96] P. J. Barendrecht, M. Bartoň, J. Kosinka, Efficient quadrature rules for subdivision surfaces in isogeometric anal-  
 1226 ysis, *Computer Methods in Applied Mechanics and Engineering* 340 (2018) 1–23.
- 1227 [97] Q. Zhang, M. Sabin, F. Cirak, Subdivision surfaces with isogeometric analysis adapted refinement weights,  
 1228 *Computer-Aided Design* 102 (2018) 104–114.
- 1229 [98] T. Takacs, Approximation properties over self-similar meshes of curved finite elements and applications to subdivi-  
 1230 sion based isogeometric analysis (Jul. 2023). [arXiv:2307.10403](https://arxiv.org/abs/2307.10403), [doi:10.48550/arXiv.2307.10403](https://doi.org/10.48550/arXiv.2307.10403).
- 1231 [99] T. Nguyen, K. Karčiauskas, J. Peters, C1 finite elements on non-tensor-product 2d and 3d manifolds, *Applied*  
 1232 *Mathematics and Computation* 272 (2016) 148–158. [doi:10.1016/j.amc.2015.06.103](https://doi.org/10.1016/j.amc.2015.06.103).
- 1233 [100] K. Karčiauskas, J. Peters, Smooth multi-sided blending of biquadratic splines, *Computers & Graphics* 46 (2015)  
 1234 172–185. [doi:10.1016/j.cag.2014.09.004](https://doi.org/10.1016/j.cag.2014.09.004).
- 1235 [101] K. Karčiauskas, T. Nguyen, J. Peters, Generalizing bicubic splines for modeling and IGA with irregular layout,  
 1236 *Computer-Aided Design* 70 (2016) 23–35. [doi:10.1016/j.cad.2015.07.014](https://doi.org/10.1016/j.cad.2015.07.014).
- 1237 [102] K. Karčiauskas, J. Peters, Refinable multi-sided caps for bi-quadratic splines, Vision, modeling, and visualization:  
 1238 26th international symposium on vision, modeling, and visualization virtual-only event September 27-28, 2021  
 1239 at the Faculty of Computer Science of the Technische Universität Dresden, German (2021) 1–8 [doi:10.2312/](https://doi.org/10.2312/vmv.20211371)  
 1240 [vmv.20211371](https://doi.org/10.2312/vmv.20211371).
- 1241 [103] K. Karčiauskas, J. Peters, Multi-sided completion of C2 bi-3 and C1 bi-2 splines: A unifying approach, *Computer*  
 1242 *Aided Geometric Design* 86 (2021) 101978. [doi:10.1016/j.cagd.2021.101978](https://doi.org/10.1016/j.cagd.2021.101978).
- 1243 [104] K. Karčiauskas, J. Peters, Least Degree G1-Refinable Multi-Sided Surfaces Suitable For Inclusion Into C1 Bi-2  
 1244 Splines, *Computer-Aided Design* 130 (2021) 102927. [doi:10.1016/j.cad.2020.102927](https://doi.org/10.1016/j.cad.2020.102927).
- 1245 [105] D. Toshniwal, Quadratic splines on quad-tri meshes: Construction and an application to simulations on water-  
 1246 tight reconstructions of trimmed surfaces, *Computer Methods in Applied Mechanics and Engineering* 388 (2022)  
 1247 114174. [doi:10.1016/J.CMA.2021.114174](https://doi.org/10.1016/J.CMA.2021.114174).
- 1248 [106] F. Buchegger, B. Jüttler, A. Mantzaflaris, Adaptively refined multi-patch B-splines with enhanced smoothness,  
 1249 *Applied Mathematics and Computation* 272 (2016) 159–172. [doi:10.1016/j.amc.2015.06.055](https://doi.org/10.1016/j.amc.2015.06.055).
- 1250 [107] M. Marsala, A. Mantzaflaris, B. Mourrain, G1 – Smooth biquintic approximation of Catmull-Clark subdivision  
 1251 surfaces, *Computer Aided Geometric Design* 99 (2022) 102158. [doi:10.1016/j.cagd.2022.102158](https://doi.org/10.1016/j.cagd.2022.102158).
- 1252 [108] M. Kapl, G. Sangalli, T. Takacs, An isogeometric C1 subspace on unstructured multi-patch planar domains,  
 1253 *Computer Aided Geometric Design* 69 (2019) 55–75. [doi:10.1016/J.CAGD.2019.01.002](https://doi.org/10.1016/J.CAGD.2019.01.002).
- 1254 [109] M. Kapl, G. Sangalli, T. Takacs, Dimension and basis construction for analysis-suitable G1 two-patch parameter-  
 1255 izations, *Computer Aided Geometric Design* 52–53 (2017) 75–89. [doi:10.1016/j.cagd.2017.02.013](https://doi.org/10.1016/j.cagd.2017.02.013).
- 1256 [110] J. Cottrell, T. Hughes, A. Reali, Studies of refinement and continuity in isogeometric structural analysis, *Computer*  
 1257 *Methods in Applied Mechanics and Engineering* 196 (41-44) (2007) 4160–4183. [doi:10.1016/J.CMA.2007.](https://doi.org/10.1016/J.CMA.2007.04.007)  
 1258 [04.007](https://doi.org/10.1016/J.CMA.2007.04.007).
- 1259 [111] B. Jüttler, U. Langer, A. Mantzaflaris, S. E. Moore, W. Zulehner, Geometry + Simulation Modules: Implementing  
 1260 Isogeometric Analysis, *PAMM* 14 (1) (2014) 961–962. [doi:10.1002/pamm.201410461](https://doi.org/10.1002/pamm.201410461).
- 1261 [112] A. Mantzaflaris, An overview of geometry plus simulation modules, in: D. Slamanig, E. Tsigaridas,  
 1262 Z. Zafeirakopoulos (Eds.), *Mathematical Aspects of Computer and Information Sciences*, Springer, Cham, 2020,  
 1263 pp. 453–456. [doi:10.1007/978-3-030-43120-4\\_35](https://doi.org/10.1007/978-3-030-43120-4_35).
- 1264 [113] T.-H. Nguyen, R. R. Hiemstra, S. K. F. Stoter, D. Schillinger, A variational approach based on perturbed eigen-  
 1265 value analysis for improving spectral properties of isogeometric multipatch discretizations, *Computer Methods in*  
 1266 *Applied Mechanics and Engineering* 392 (2022) 114671. [doi:10.1016/j.cma.2022.114671](https://doi.org/10.1016/j.cma.2022.114671).